Université Abou Bekr Belkaid
Tlemcen Algérie

جامعة آبي بكر بلقايد

تلمسان الجزائر

République Algérienne Démocratique et Populaire

Université Abou Bakr Belkaid– Tlemcen

Faculté des Sciences

Département de Physique

LPT
Tlemcen

Laboratoire de physique théorique

Mémoire de fin d'études

Pour l'obtention du diplôme de Master en Physique

Option : Physique Théorique

Thème

Application of the Monte–Carlo method to the agglomeration problems

Présenté par :

Mlle Somia BELALIA

Le mercredi 27 Juin 2018

Devant le jury composé de :

- **Pr** Smain BEKHECHI   .... Président
- **Dr** Djilali AMEUR   .... Encadreur
- **Dr** Joanna DIB   .... Co-Encadreur
- **Pr** Zinelabidin BENTALHA   .... Examinateur

Année universitaire : 2017-2018

GRATITUDE

DEDICATION

To my parents, my father who always told us that learning never stops, to my mother who told me that every night has a new dawn. My dear parents, I'm dedicating you this work which without you wouldn't have been achieved.

To my sisters Sihem and Sanaa, with whom I spent the best days of my life throughout my study journey from college to university studies and even before.
To my brothers Boumedienne and Lotfi, the best thing happened in my life.

To my grandparents in the other world.

To all my friends.

To the ones I love.

Table of contents

Table of figures

List of tables

Chapter 1

Introduction- *Green chemistry challenge*

Over the years, because of fast growth of population and industrial activities, we have increasingly polluted our waters. Conventional water treatment processes become indequate with the identification of new contaminants in the water. To overcome these challenges, a particular emphasis is accorded to the implementation of environmentally, eco-friendly and less-energy technologies for waste water treatment processes. In order to provide a sustainable development and to avoid the negative impacts on our environment, green chesmistry science and technology offers economically alternatives for chemical water treatments. These techniques are carried out by adding organic polymers instead of inorganic coagulants in order to meet the green treatment goals by taking into account the protection of public health and the environment and combining maximum efficiency with minimal toxicity.
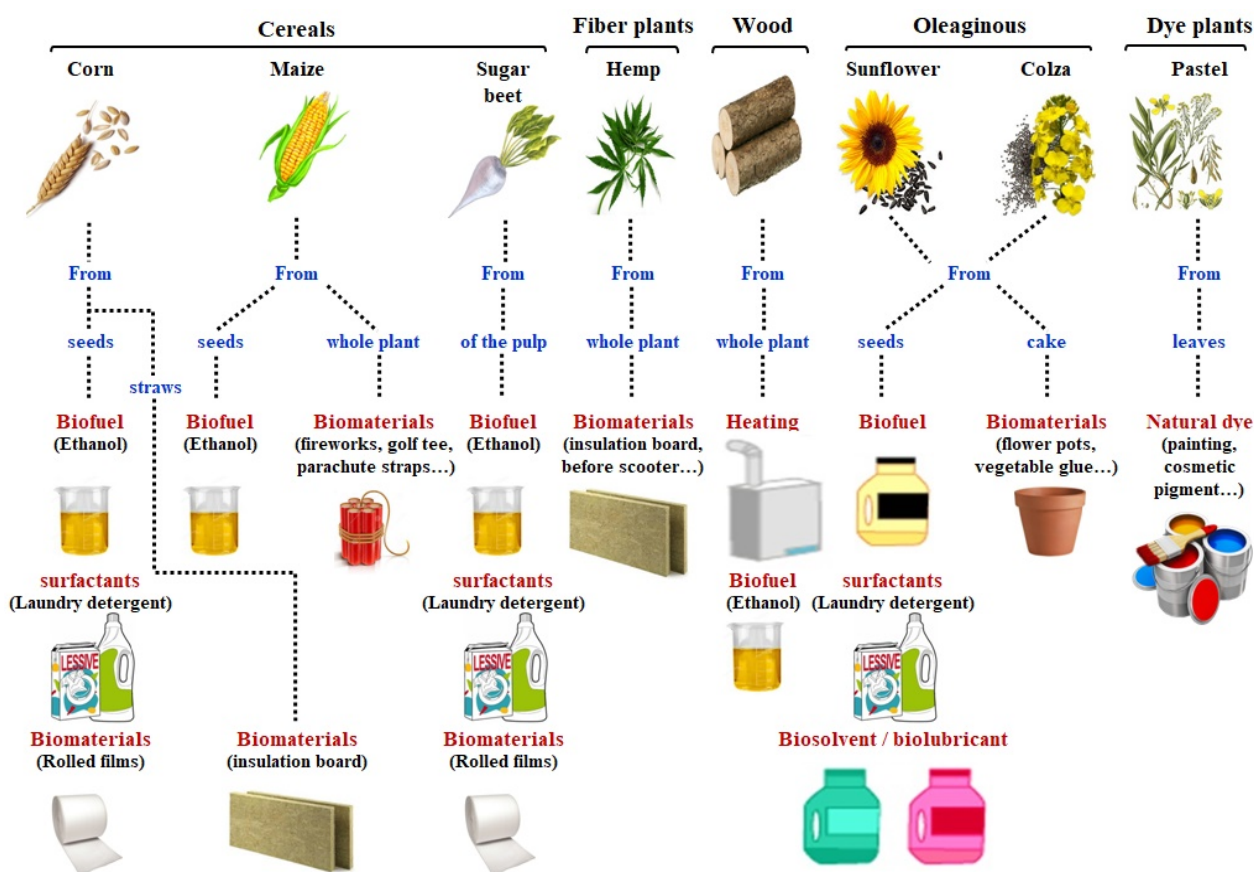
FIGURE 1.1 – Green chemistry. (www.faiteslepleindavenir.com)

Different types of waste water treatment exist around the world, they vary according to the types of contaminants present in the water. In this work, we focus our attention on stabilized colloidal suspensions that show no sedimentation rate despite the existence of density variation between the two phases. The conventional methods of solid-liquid separation for urban waste process water treatment cannot be used directly on stabilized colloids suspensions. These anionic particles of sizes varying between 10^{-11} and 10^{-9} m, are small enough to stay suspended for a long period of time. Actually, colloids have a surface activity which has an appreciable influence on the properties of the aggregate. This phenomena governs the stability of colloidal suspensions which results from the balance between the attractive energies of Van der Waals, which favor aggregation, and the electrostatic repulsion energies. In order to destabilize these

colloids, we should promote their agglomeration by reducing their electrostatic repulsion energies. Two mechanisms are mainly involved: coagulation and floculation which are carried out by choosing alternative substances with low volatility. These processes employ substances that are weakly toxic for humans and without consequences for the environment. These mechanisms depend on the aggregation rate between particles and are modelised by the Monte Carlo method for solving Smoluchowski's coagulation equation, a population equilibrium equation which describes in statistical chemical physics the agglomeration. The Smoluchowski equation is of universal use in the fields of Colloid chemistry, Aerosol dynamics and Nanotechnology Science. It is to say that the collision rate per unit length is due to the Brownian motion and the particle agglomeration rate depends on the particles contact probability and the effectiveness of the latter. Numerical resolution of the Smoluchowski equation is obtained employing the Monte Carlo technique and its alternatives methods.

In this work, we solve the Smoluchovsky equations and study the number concentration of coagulated particles, which decreases with the growth of th particle size. Finaly, we compare our numerical results to the analytical solutions and we show that the method seems to be more accurate approximating the first moment.

Chapter 2

Colloids

Contents

Colloids are particles of sizes varying between 10^{-2} and 1 μm and are generally negatively charged. Actually, colloids have a surface activity which has an appreciable influence on the properties of the aggregate. This phenomena governs the stability of colloidal suspensions which results from the balance between the attractive energies of Van der Waals, which favor aggregation, and the electrostatic repulsion energies.

The nature of colloids is related to their origins and mechanisms that contribute to their formation. In general, the different types of colloids are hardly present in the pure state in the media but rather associated with compounds to form particles of colloidal size. The most easily found form are those from soil such as Ox iron and/or aluminum hydroxides and aluminosilicates. High molecular weight organic matter, bio-colloids and bacteria are also found. Due to the spreading of waste or fertilizers, there is also a possibility to find colloids of carbonated and phosphatic nature. As mentioned above, the removal of these colloids strongly depends on their surface charge properties and sizes. Colloids can also be classified as electronegative and hydrophilic, such as organic macromolecules, humic or non-humic substances and/or electropositive and hydrophobic such as metal oxides and clay minerals.

2.1   Double layer theory
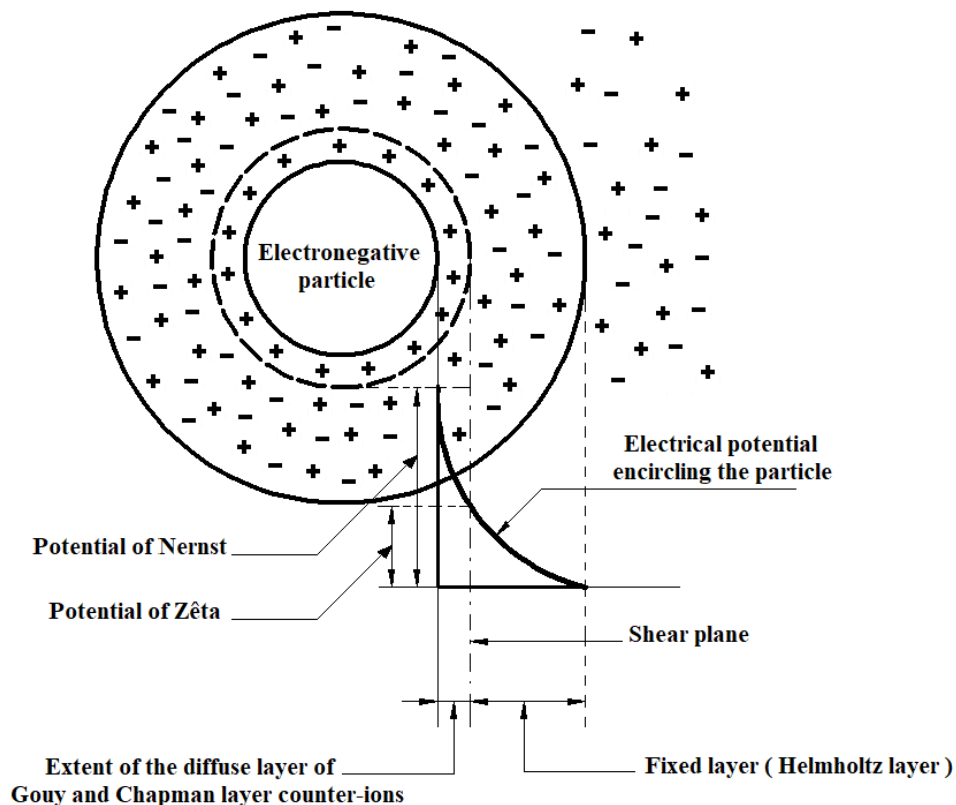
FIGURE 2.1 – Colloid. (hmf.enseeiht.fr)

In fact, the colloid moves in the solution with part of its electric double-layer repulsion. The first layer is fixed to the colloid surface and the second is more diffuse. The potential difference

between the first layer and the solution is called the zeta potential which governs the displacement of the colloids and their mutual interaction. To destabilize the suspension and promote the agglomeration of the colloids, it is necessary to reduce the zeta potential so that the Van der Waals forces become dominant again. This kind of aggregation is known as coagulation. This destabilization is achieved by coagulation polymers of Low Molecular Weight with a high cationic charge in order to neutralize the negative charges of the colloids.

After colloidal suspensions have been destabilized, flocculants polymers are frequently used because of their very High Molecular Weight, i.e. high degree of monomer polymerization. These flocculants are extremely effective in bonding the micro-flocs formed during coagulation by using long polymer chains. The polymer chain in solution is partially adsorbed on a particle beyond its double layer and when other particles are close enough, the elongate chain is adsorbed on its surface and creates bridging between the two particles. Various theories explain this phenomenon [1] :

Helmoltz theory : The neutrality of the whole (the surface of the colloid and the positive particles called ions) is realized when the latter comes into full contact with the surface of the colloid (fixed layer).

Gouy-Chapman theory : The neutralization can be obtained at a greater distance, this is done when the colloid is unequally surrounded by a layer of positive ions (diffuse layer).

Stern's theory : Stern took into consideration the previous theories and discovered the double layer formation theory. The first remains with the particle which causes a rapid decrease, and the second is more diffuse which explains the slow decrease of the potential.

2.2 Colloid characteristics

2.2.1 Thermodynamic potential

called also the **Nernst potential**. It lies on the colloidal surface.

We have :

$$\Delta G_r = \Delta \mathring{G}_r + RT \ln Q$$

ΔG_r is The standard free reaction enthalpy.

where Q is the reaction quotient.

Since

$$\Delta \mathring{G}_r = -nf\Delta E$$

We obtain :

$$-nf\Delta E = -nf\Delta \mathring{E} + RT \ln Q$$

11

The factor RT/f often appears in electrochemistry its value is $2.5693. \, 10^{-2}$ J.C^{-1}

Then dividing the two membranes by the following term $-nf$, we obtain the Nernst equation :

$$\Delta E = \Delta \mathring{E} - \frac{RT}{nf} \ln Q.$$

Nernst's equation allows us to predict the variation of electromotive force with concentration and pressure.

2.2.2 Zeta potentiel

The Zeta potential is also called the **_electrokinetic potential_**. Its measurement is carried out at the limit between the part of the solution which moves during the displacement of the particle and the part of the solution which changes direction independently of the particle, this plane is called the shear plane.

Water contains suspended solids, impurities we would like to dispose of. Due to the repulsive forces that the colloids exert between them, these particles are stable enough to stay suspended which makes the sedimentation operation and the coagulation flocculation mechanisms impossible to realize. In this context, we should promote the reducing of the repulsion forces between particles aiming to neutralize the negative charges of colloids by the addition of coagulants with cations, which decreases the potential until it becomes negligible.

The optimal dose is the cause for which the Zeta potential becomes zero (which is the purpose of our work), the opting for an optimal dosage is done by monitoring the potential Zeta depending on the rate of coagulant, we can choose the best coagulant by doing a test of several coagulant to know which one is the most good.

$$\boxed{Z = k\mu m_e / \varepsilon}$$

where

- k is the function of the diameter of the particle,

- μ is the dynamic viscosity (Pa. S),

- m_e is the electrophoretic mobility ($\mu.s^{-1}.v^{-1}$),

- ε is the dielectric constant of the medium. Here is the measuring device "Zetameter".
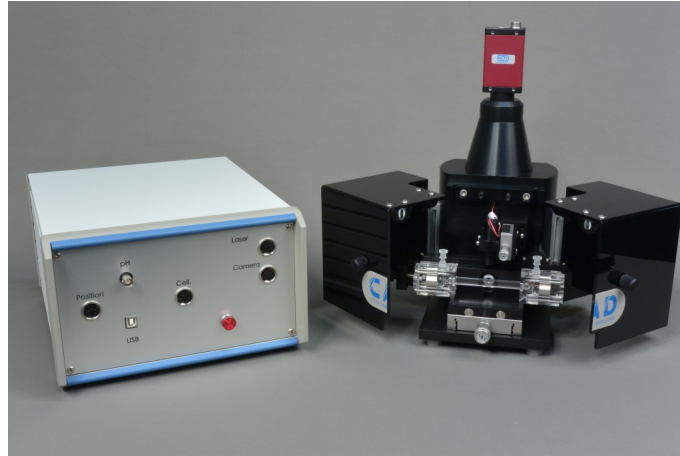
FIGURE 2.2 – Zetameter. (lavallab.com)

Two main forces which occure when two particles come into contact:

The ***attractive force of Van Der Waals:*** The origin of attraction between a temporary dipole and the corresponding induced dipoles are due to the Van Der Waals forces, which is explained in the London theory. The Van Der Waals forces can take different forms and take the order of $1/r^7$, which explains the speed of decrease related to the distance.

The ***electrostatic repulsion force:*** Due to the Coulomb's law, the Coulombic force depends on the dielectric constant of the medium, i. e. more the solvent is polar, more the force is weaker.
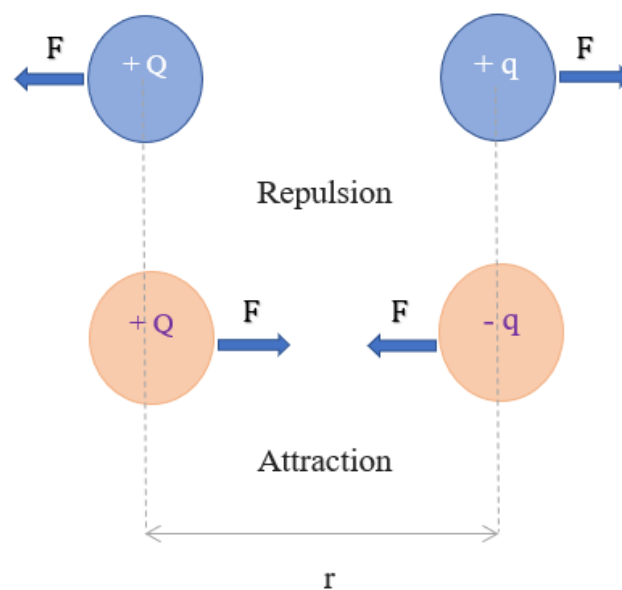
FIGURE 2.3 – Coulomb's law.
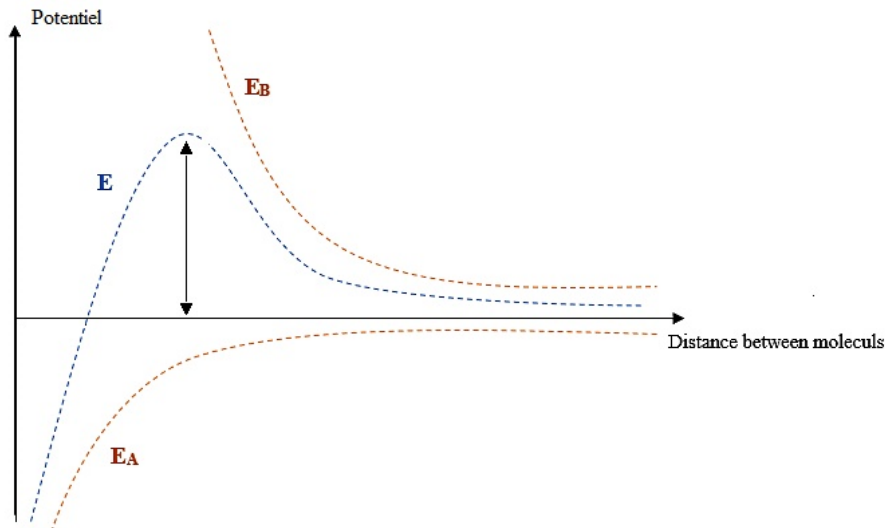
FIGURE 2.4 – The relation between the Van Der Waals and the electrostatic forces.

where

- E_B is the potential derived from the electrostatic repulsion force,

- E_A is the potential derived from the attractive force of Van Der Waals,

- E is the resulting potential,

- $\updownarrow$ is the energy barrier.

In general, the efficiency of a polymer depends on the molecular chain length, because more the chain is longer more the probability of creating bridging is greater. Two mechanisms are mainly involved: coagulation and floculation. The presence of very small diameter particles such as colloids, is responsible of the color and turbidity of the surface water. Their removal is not possible via settling because of their low sedimentation rate. Coagulation can neutralize their electrostatic charges repulsions to allow their aggregation by destabilizing it. Flocculation works on their agglomeration in aggregates removed by decantation and/or fit.
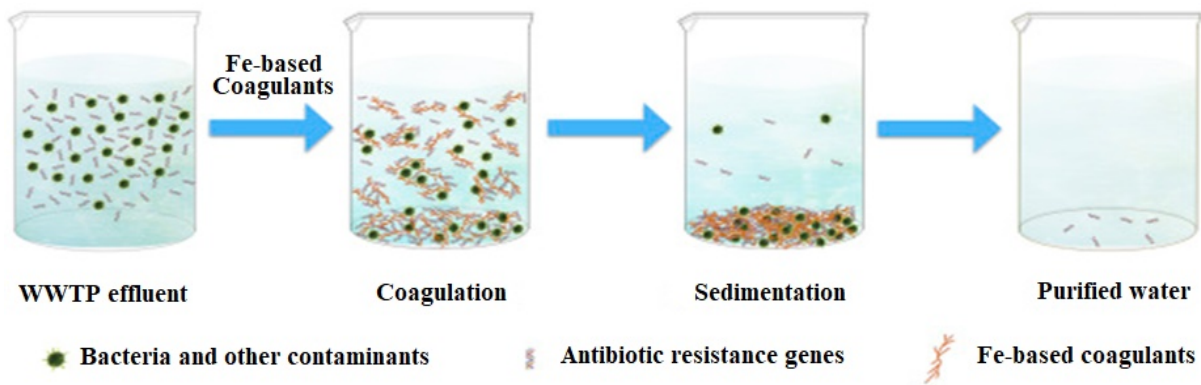
FIGURE 2.5 – The coagulation flocculation process. (slideplayer.com)

Colloids have very important characteristics. Their surface/volume ratio results from the adsorption properties of the ions present in the water. This explain the existence of electrically charged surface, often charged negatively, creating inter-colloidal repulsion forces. Flocculation is due to the aggregation process or macromolecules adsorbed simultaneously on two or more particles, establishing between them a set of bridges. When aggregation is carried out following the presence of oppositely charged polymer particles, neutralization of the surface charge obtained after adsorption can not be neglected. Aggregation is the result of the joint action of the two previous phenomena. Bridging comes from the critical arrangement of the adsorption rate and reconformation of the polymer at the interface and the effective particle collision rate.

We are considering in our study two phenomena: coagulation and flocculation.

2.3 Coagulation

Coagulation is the set of physico-chemical phenomena by which certain constituents of very small sizes called colloidal particles of a stable suspension groups together to obtain a more impactful mass. We can find it in several domains like the formation of large structures at astronomical scales (galaxies), we can also mention the planets and the stars by accretion in astrophysics. Coagulation can also be called *aggregation*, *coalescence* or *nucleation*[2].

2.3.1 Principle of coagulation

There are two steps to the aggregation process:

- Firstly, the addition of a so-called "coagulant" reagent causes the decrease or even the cancellation of the stability of the colloidal suspensions.

- Secondly, after destabilization, the particles come into contact with each other following mechanical agitation (in the process of water treatment). The difference in electrical charge between the particle and the solution causes an ionic layer.

From a thermodynamic point of view, the DLVO theory [17] can define the interaction between an attraction energy that comes from the Van Der Waals forces and another repulsive energy from the ionic double layers surrounding the particles.

2.3.2 Coagulation mechanism

Coagulation aims to cancel the Zeta potential in order to ensure a decreasing of the attractions forces, the thing that most trouble the coagulation phenomenon. This is achieved when the attractive forces of Van der Waals become dominant. Therefore the increase of the electrolyte concentration becomes an essential stage since it is the operation which compresse the double ionic layer.

Among the coagulants most often used are: *Aluminum Sulphate, Sodium Alumina,Ferrous Sulphate, Chlorine, Ferric Sulphate, Ozone*, etc.

2.4 Flocculation

Flocculation appears in astrophysics (stellar fragmentation), in chemistry (the degradation of large chains of polymers), the flocculation of DNA in biology and many other areas [2].

The second step in the clarification of water is flocculation, it is divided into two phenomena [3]:

• Peri-kinetic Flocculation: related to the thermal agitation mostly related to the Brownian diffusion. It favorise the formation of micro-flocs.

• Ortho-kinetic flocculation: related to the dissipated energy aiming to the formation of big flocs. The probability of particle encounter is connected. The stirring speed acts on the probability of particles encounter, but it is not possible to increase it excessively. Indeed, if it is too high, the formed flocs undergo a mechanical shear causing their destruction and they seldom reform themselves. Flocculation is therefore favored by a fairly low stirring speed which gently causes the flocks to meet.

2.4.1 Principle of flocculation

After the particles destabilization has been performed, the colloidal particles agglomerate with each other. The difference in stirring speed causes an increase in the probability of particles encounter.

2.4.2 Flocculants

The floc formed by the agglomeration of several colloids may not be large enough to decant or to dehydrate at the desired rate. The use of a flocculant is then necessary. It collects all the floc particles in a net, building a bridge from one surface to another and binding each particle to form large clusters [23]. The time between additions of coagulant and flocculant is crucial. Indeed, a flocculant is generally effective only when the coagulation phase is complete.

To choose flocculants, we consider the size, cohesion and settling speed of the flocs.

As for coagulants, the treatment rate to be implemented is given by a flocculation test. We employ [8]:

- Mineral polymers such as activated silica (SiO_2), generally associated with aluminum sulphate in cold water.

- Natural polymers extracted from animal or vegetable substances : starches, alginates (obtained from marine algae).

- More recently synthesized polymers have significantly changed the performance of flocculation. They often lead to a much lower volume of sludge.

2.5 Parameters influencing coagulation and flocculation

We consider six important parameters that influence the coagulation-flocculation mechanisms studied [23]:

2.5.1 Temperature

The temperature has an appreciable influence on the viscosity of the solution, which is why raising or lowering the temperature prevents the operation.

2.5.2 Agitation

The operation begins with a rapid stirring at the beginning which promotes the dispersion and homogenization of the water, even if intense agitation can prevent the agitation of the particles. Then we move to slow agitation, it allows us to cause contact between the particles to form decanter flocs.

2.5.3 PH

PH is one of the most influential parameters in the coagulation process, and the same goes for flocculation. It is very difficult to determine the optimum pH value for coagulation and flocculation processes, since they include different phenomena in different pH ranges. The best thing to do would be to find a compromise between coagulation pH (acid) and pH of flocculation (basic).

2.5.4 The nature of colloids

The characteristics of the colloids in terms of charge and the ability to interact with other similar particles (electronegativity) play a very important role in coagulation.

2.5.5 Coagulant

Our choice of coagulant can influence either positively or negatively the treatment of water. Two main types of coagulants:

- Minerals such Asiron or Aluminum salts.

- Organic such as Polyamine, PolyDADMAC, ...

In our work we focus on the PolyDADMAC [22] which was studied and prepared for the first time by Pr. George Bulter. Because of its solubility in water, it was very useful in contrast to other polysynthetics. Its structure was determined in 2002 by the NMR studies. PolyDADMAC is used in waste water treatment as a primary organic coagulant that neutralize the negative charges of colloids and reduce the volume of sludge compared to inorganic coagulants. It has a great effect on coagulation and flocculation of organic and inorganic particles such as clay, bacteria and viruses. The organic polymer removes naturally occurring organic materials such as humic acids at a high concentration, reducing the number of disinfection byproduct precursors and color.

2.5.6 Color

The particles that cause the color of water are usually larger than those causing turbidity, they have a diameter greater than 3.5 nm, while the colloids diameter that causes turbidity are very small.

2.6 Brownian motion

Robert Brown was the first researcher who observed the Brownian movement in 1827, Brown's observation of pollen grains under the microscope, shows that particles move in a bizarre way, grains eject small particles into the water, the astonishing thing is that these particles do not stop moving and move in all directions as if something jump them. Brown has redone the same experience on different types of particles and realize that these molecules moved due to a certain thermal agitation [15].

From the grains observation, Brown noticed that these particles do not follow a strategy which means that the Brownian movement is irregular and unpredictable. He also noticed that it is not possible to concentrate on a single particle or molecule and really knowing its way because of its rapidity and random displacement, Brown rearked also that as long as the temperature of the medium is higher, the viscosity is low and the particle size is small, the variation of the movement is more significant and will never be negligible. From these observation, it was clear that this movement was the result of molecules shocks with the particle.

Thermal agitation is the microscopic phenomenon that describes the movement of particles relative to each other, it also describes the heat storage of particles, this stall is defined itself in the form of molecular stirring. Now lets take particles that meet with molecules, we can directly see that during the molecules displacement, the collision operation begins immediately with the particles. This leads us to the amount of motion that will be introduced by the molecule itself

when it exerts a force on the paticule with each collision. While another random force will be applied to the particle in its direction and amplitude, this happens after each collision. Moreover, the viscosity of the fluid causes an indefinite to this particle which itself causes a stop to their move [14] [24].

The amplitude of the Brownian motion has an inverse relationship with the size of the particle. In fact the increase in particle size causes numerous collisions with molecules, as well as an increase in particle masses, which leads to a shock that causes a small displacement. The addition of these two variations leads to a poor displacement for large particles. A statistical property which explains this phenomenon is called the *law of large numbers*, it states that if the number of random shocks increases, the sum of shocks converges to zero, the reason why it is not possible to see this phenomenon or this movement on a macroscopic scale [18] [24].

2.6.1 The model of Einstein (1905)

In 1905, Einstein provided a quantitative description of the Brownian motion. His predictions were then experimentally verified by Jean Perrin a few years later. The mean quadratic displacement described above, corresponds to a diffusion process, i.e if a particle is at the position $x = 0$ initially, it will be after a time t at a position x [19]:

$$\langle x^2 \rangle = 2DT,$$

where $\langle x^2 \rangle$ represents the mean quadratic displacement (the brackets indicate the mean value of x^2 when repeating the experiment several times), and D is a diffusion coefficient.

Einstein has established an expression of the diffusion coefficient that holds for spherical radius particles R:

$$D = \frac{k_B T}{6\pi \eta R},$$

where

- k_B is a constant (Boltzmann constant).

- T is the temperature.

- η is the the viscosity of the liquid.

- R the particle radius.

In this formula, we can see that the mean quadratic displacement increases with temperature and decreases with particle size, in agreement with the previous statistical arguments. The expression of the diffusion coefficient is particularly interesting because it also involves the viscosity of the liquid. $6\pi \eta R$ is actually the coefficient of friction of the particles in the liquid. Thus, in the diffusion process, the thermal fluctuations ($k_B T$) of the molecules increase the diffusion, whereas the friction, which tends to slow down and stop the particles after they under go a random force decreases it [19].

2.6.2 The model of Langevin (1908)

Langevin was interested in the mechanical approach that allows him to better manipulate this phenomenon, therefore he proposed a method that allows to preserve it. In fact, instead of treating all the equations, we can simply employ the law applied to the average values of speed and acceleration. Langevin was able to make a balance of the average force which are exerted on a particle. In the first place he spook of a force $\vec{F}$, which following collisions with atoms or particles, fluctuations of the trajectories are translated by it. The temp duration of these fluctuations is really short compared to the duration that the Brownian movement does [20]. We note that the average value of $\vec{F}$ is zero under homogeneous and isotropic conditions. Moreover if the time duration between two instants t_1 and t_2 is smaller than the time scale of the fluctuations, then the values of $\vec{F}$ at these two moments will be independent random variables, which leads us to say that the average magnitudes $< F(t) >$ and $< x(t) >$ are correlated:

$$< x(t)F(t) >=< x(t) >< F(t) > .$$

Another force has been studied is the friction force of a fluid is given by: $-m\gamma\vec{v}$. It reflects the dissipation due to friction.

Equipped with this balance of forces, we can therefore put Langevin's equation: $md\vec{v}/dt + m\gamma\vec{v} = \vec{F}$, neglecting of gravity.
The quadratic value is $< v^2(t) >= kT/m$, in a one-dimensional model, with k, the Boltzmann constant, taking into account that the particle is in thermal equilibrium with its environment.

The solution of the Langevin equation is given by:

$$< d(x^2(t)/2)/dt >=< d(x^2(0)/2)/dt > * \exp{-\gamma t}) + kT/m\gamma$$

By examining this solution and integrating it with time, we deduce at least two things:

• For t tending towards 0, that is to say for the small times before the interval of the shocks, between the molecules of liquid and the particle, we will have a ballistic case, which corresponds to a classical solution of trajectory, with $< x^2(t) >$ tending to $2(v_0 * t)$.

• For t large in front of the shock interval, $< x^2(t) >$ tends to $2(kT/m\gamma)t$. Here we recognize the diffusion coefficient D, already encountered in Einstein's model.

Chapter 3

Smoluchowski equations

Contents

For a given polymer, bridging mainly depends on two parameters : the number of sites available for adsorption on the colloids surface and the rate of polymers agglomeration. One can consider that the probability of two polymer chains fusion is proportional to their lengths sum [13].

The beginning of the classical understanding of colloidal aggregation stem from the work of Smoluchowski on coagulation processes in colloids, a population equilibrium equation which describes in statistical chemical physics the agglomeration which follows from the assumption that the collisions are binary and that fluctuations in density are sufficiently small so that the collisions occur at random, i.e. the evolution of the temperature of the coagulation particle density of size i at time t.

The Smoluchowski equation is of universal use in the fields of Colloid chemistry, Aerosol dynamics and Nanotechnology Science. It is to say that the collision rate per unit length is due to the Brownian motion and the particle agglomeration rate depends on the particles contact probability and the effectiveness of the latter. Numerical resolution of the Smoluchowski equation is obtained employing the Monte Carlo technique and its alternatives methods.

The Smoluchowski's equations are given by [11]:

$$\frac{\partial c}{\partial t}(i,t) = \frac{1}{2}\sum_{j=1}^{i-1} K(i-j,j)c(i-j,t)c(j,t) - \sum_{j=1}^{\infty} K(i,j)c(i,t)c(j,t), i \in \mathbb{N}^*, t \geq 0, \qquad (3.1)$$

$$K(i,j) = i+j \text{ and } c(i,0) = c_i(0) = \begin{cases} 1 & \text{if } i = 1, \\ 0 & \text{else}. \end{cases}$$

System (3.1) is deduced for a set of particles 1, 2, 3,... or any other whole mass at time t, where c(i,t) denotes the number of polymers of length i at time t. Two particles of length i and j merge into a single particle of length (i + j), their probability of fusion is K (i, j) which is the coagulation Kernel and it is proportional to the density of these two particles. Physically, we assume that the number and total length of the polymers are finite and that K(i, j) is nonnegative and symmetric. The first term on the right-hand side represents the rate of agglomeration of polymers of length k by agglomeration of any polymers pair of length i and j, such that i+j = k. The second term accounts for the loss of polymers of length k by agglomeration with any other polymers chains. The variance of c(i, t) is given by the melting of particles of lengths i and j and by the disappearance of particles of sizes (i + j) following a fusion with another particle.

Moreover, the coalescence $(i,j) \longrightarrow (i+j)$ has the same probabilitiy as the coalescence $(j,i) \longrightarrow (i+j)$, therefore The average number of coalescence $(i,j) \longrightarrow (i+j)$ per unit of time and volume [2] is given by $K(i,j)c(i,t)c(j,t)$.

Rather than approximating the density, we shall approximate the mass density which satisfises the following equation:

$$\frac{\partial \tilde{c}}{\partial (t)}(i,t) = \frac{1}{2}\sum_{j=1}^{i-1}\tilde{K}(i-j,j)\tilde{c}(i-j,t)\tilde{c}(j,t) - \sum_{j=1}^{\infty}\tilde{K}(i,j)\tilde{c}(i,t)\tilde{c}(j,t), i \in \mathbb{N}^*, t \geq 0, \qquad (3.2)$$

$$\tilde{c}(i,0) = \tilde{c}_i(0)$$

where

$$\tilde{c}(i,t) := ic(i,t) \text{ and } \tilde{K}(i,j) := \frac{K(i,j)}{j}$$

An analytical solution is given by [7] [11]:

$$c(i,t) = e^{-t}\frac{i^{i-1}}{i!}(1-e^{-t})^{i-1}e^{-i(1-e^{-t})}, i \in \mathbb{N}^*, t \geq 0$$

3.1 Coagulation kernel

In 1928, *Müller* proposes a differential integral equation of the Smoluchowski equation which is known under the *Smoluchowski's continuous coagulation equation*:

$$\frac{\partial c(i,t)}{\partial t} = \frac{1}{2}\int_0^i K(i-j,j)c(i-j,t)c(j,t)dj - \int_0^{\infty} K(i,j)c(i,t)(j,t)dj \qquad (3.3)$$

where

- c(i, t)dj is the particle number whose volume is between i and i + dj at time t.

- K(i, j) is the collision kernel for two particles of volumes i and j.

In the free molecular regime, the collision kernel was derived from the gas kenetic theory [12]:

$$K(i,j) = B_1(\frac{1}{i} + \frac{1}{j})^{1/2}(i^{1/3} + j^{1/3})$$

where

- $B_1 = (\frac{3}{4\pi})^{1/6}(6k_bT/\rho)^{1/2}$.

- k_b is the Boltzmann constant.

- T is the gas temperature.

- ρ is the mass density of particules.

In a dilute gas-phase, the collision kernel take the following equation:

$$K = \sqrt{\frac{\pi k_B T}{2}} (\frac{1}{m(i)} + \frac{1}{m(j)})^{1/2} (d(i) + d(j))^2$$

In the specific dimension of the Clusters, as in diffusion-limited aggregation:

$$K = \frac{2k_B T}{3\eta} (i^{1/l_1} + j^{1/l_2})(i^{-1/l_1} + j^{-1/l_2})$$

In the reaction-limited aggregation:

$$K = \frac{2k_B T}{3\eta} \frac{(ij)^\gamma}{W} (i^{1/l_1} + j^{1/l_2})(i^{-1/l_1} + j^{-1/l_2})$$

where

- l_1, l_2 is the Fractal dimension of the clusters.

- W is the Fuchs stability ratio.

- η is the continuous phase viscosity.

- γ is the exposent of the product kernel.

An analytical solution exist only when the Kernel coagulation is represented in this three forms:

- K = 1 is the constant kernel.

- K = i+j is the additive kernel.

- K = ij is the multiplicative kernel.

3.2 Moments

In 2008, Yu et al proposed the Taylor expansion method of moments that has been used in different studies because of its simplicity and reliable accuracy, a new variable has been find following studies of the asymptotic behavior of ordinary differential equations [5].

$$g = \frac{m_0 m_2}{m_1^2}$$

where m_0 m_1 and m_2 are the three first moments.

The zeroth moment m_0 represents the particle number concentration, which decreases with the growth of th particle size. The first moment m_1 remains constant and the second moment m_2 is usually used as an index to characterize the total light scattered, wich increases with the growth of particle's size and polydisperity [6].

The Taylor expension method of moments is introduces in solving (3.1) with the closure model for the k-th moment [5].

$$m_k = (\frac{u^{k-2}k^2}{2} - u^{k-2}\frac{k}{2})m_2 + (-u^{k-1}k^2 + 2u^{k-1}k)m_1 + (u^k + u^k\frac{k^2}{2} - 3u^k\frac{k}{2})m_0 \qquad (3.4)$$

where u is the Taylor expansion point, defined to be m_1/m_0.

In this work, we compute the analytical solution up to time T=2 for different time steps varying from $\Delta t = \frac{T}{100}$ to $\Delta t = \frac{T}{1000}$ and for several particle numbers varying from $N = 10^4$ to $N = 10^5$ and we compare the exact moments to the approximate moment of order 0 which corresponds to the number concentration of coagulated particles which decreases with the growth of the particle size :

$$M_{0,N}(t) = \sum_{k=1}^{N} \frac{1}{i_{N,n}(k)} \text{ and } M_{2,N}(t) = \sum_{k=1}^{N} i_{N,n}(k)$$

to the exact moments of order 0 and 2 over the interval [0,T]:

$$M_p(t) = \sum_{i=1}^{\infty} i^p c(i,t) = \sum_{i=1}^{\infty} i^{p-1} \check{c}(i,t)$$

where $M_0(t) = e^{-t}$ and $M_2(t) = e^{2t}$.

3.3 Introduction to the Monte Carlo methods

Monte Carlo simulation is a method of estimating a numerical quantity that uses random numbers. It is always difficult to know who among the researchers Von Neumann, Ulam, Fermi and Metropolis has named it in reference to gambling in casinos during the Manhattan project that produced the first atomic bomb during the Second World War [1].

The Monte Carlo methods designate any method of calculating probabilistic techniques, using random processes in order to find solutions to numerical value calculation problems. Moreover, it gives a statistical support. Monte Carlo simulation has the dual advantage of being simple to use and can be applied to a very wide range of problems. It is used in finance to determine when to raise an option on a financial asset, in insurance to assess the amount of a premium, in biology to study intra and intercellular dynamics, in nuclear physics to know the probability that a particle crosses a screen, in telecommunications to determine the quality of service, or generally to determine a system's reliability, availability or average time to failure. However, it is necessary to pose the problem, to model it so that the quantity to be sought will be expressed as the expectation of a random variable X, denoted E(X) [4].

A random variable is the result of a random experiment employed to estimate a purely deterministic quantity, for example a surface or an integral, by artificially constructing a random variable to be reduced to the calculation of an average. The use of this methods covers all areas

of physics, mathematics, molecular and genetic biology as well as finance.

Monte Carlo is less accurate than the known integration methods such as the Simpson, Romberg and trapezium method. Since the Monte Carlo method is based on the principle of the random number generator, it decreases the precision of calculation while it's really powerful in calculating multiple integrals.

3.3.1 Strong law of large numbers

We call sample mean or empirical mean the statistic written X_n defined by [15]:

$$\bar{X}_n = \frac{1}{n} \sum_{i=1}^{n} X_i \tag{3.5}$$

represents the empirical average or average of the sample.

Theoreme 3.1. *The empirical average $\bar{X}_n$ of a sequence of identically distributed independent random variables $(X_n)_n$, has a values in $\mathbb{R}^d$, $d \in \mathbb{N}$. It is almost convergent in $\mathbb{L}_1$ towards the common expectation of X_i when $n \longrightarrow \infty$. We also note that it is integrable, i. e:*

$$P\left(\frac{1}{n} \sum_{i=1}^{\infty} X_i \longrightarrow \mathbb{E}(X_n)\right) = 1.$$

3.3.2 Principle of the MC method

By using iid realizations of a law easy to simulate, we consider an integrable function compared to the Lebesgue's measure on [a, b] $g : [a, b] \longrightarrow \mathbb{R}$ and we calculate the following integral ([15], [21]):

$$I = \int_{[a,b]} g(x)dx.$$

Since X is a random variable of density f_x, we write I in the form of an expectation:

$$I = \mathbb{E}(g(x)) := \int_{\mathbb{R}} g(x)f_x dx$$

with $f_x(x) = \frac{1}{b-a} 1_{[a,b]}(x)$.

The idea is to produce a sample $(x_1, x_2, .., x_n)$, X's law on [a, b], then calculate a new estimator of :

$$G = \mathbb{E}(g(X))$$

which is the Monte Carlo estimator.

From the empirical averag,e one can build the Monte Carlo estimator:

$$g_n = \frac{1}{n} \sum_{i=1}^{n} g(x_i)$$

For n big enough, we obtain:

$$\frac{1}{n}\sum_{i=1}^{n} g(x_i) \simeq \mathbb{E}(g(X)).$$

3.3.3 Error and convergence

The notion of error remains indispensable in mathematics. In fact, this tool allows us to study the accuracy of a method and to control tolerances and limits. Therfore, we define the notion of interval of confidence [3].

For the same variable X and the same draw X_1, X_2, ... , X_n, ... , the error of the Monte Carlo estimator n is defined by the following quantity [15] [9]:

$$\epsilon_n = \mathbb{E}(X) - \frac{1}{n}(X_1 + X_2 + ... + X_n)$$

The asymptotic behavior of this error is well described by the central limit theorem which determines the law of $\sqrt{n}\epsilon_n$ for n large enough.

Theoreme 3.2. *Central limit theorem. Let us consider a sequence of identically distributed independent random variables of finite expectation $E(X_1) < +\infty$ and positive variance Finite σ^2. Let's put $S_n = X_1 + X_2 + ... + X_n$, so:*

$$\frac{S_n - n\mathbb{E}(X_1)}{\sigma\sqrt{n}} \xrightarrow[n\to\infty]{L} \aleph$$

where $\aleph$ is a reduced centric Gaussian random variable.
By a simple calculation, we show :

$$\frac{\sqrt{n}}{\sigma}\epsilon_n = \frac{\sqrt{n}}{\sigma}[\mathbb{E}(X) - \frac{1}{n}S_n] = \frac{\sqrt{n}}{\sigma}\mathbb{E}(X) - \frac{1}{\sigma\sqrt{n}}S_n = -\frac{S_n - n\mathbb{E}(X)}{\sigma\sqrt{n}}$$

Since the Gaussian variables are symmetrical and by the previous theorem, we get:

$$\frac{\sqrt{n}}{\sigma}\epsilon_n \xrightarrow[n\to\infty]{L} \aleph(0,1).$$

3.3.4 Confidence interval

In the previous section, we saw that the variable $\sqrt{n}\epsilon_n N$ converges asymptotically to a Gaussian centered reduced, i. e for all Borelian A, we have [3]:

$$\mathbb{P}(\frac{\sqrt{n}}{\sigma}\epsilon_n \in A) \to_{n\to\infty} \int_A \frac{1}{\sqrt{2\pi}} \exp^{\frac{x^2}{2}} dx$$

Moreover for A = [-a, a], we obtain:

$$\lim_{n\to\infty} \mathbb{P}(-a < \frac{\sqrt{n}}{\sigma}\epsilon_n < a) = \int_{-a}^{a} \frac{1}{\sqrt{2\pi}} \exp^{\frac{x^2}{2}} dx$$

that is to say:

$$\lim_{n \to \infty} \mathbb{P}(-a\frac{\sigma}{\sqrt{n}} < \epsilon_n < a\frac{\sigma}{\sqrt{n}}) = \int_{-a}^{a} \frac{1}{\sqrt{2\pi}} \exp^{\frac{x^2}{2}} dx$$

From here, we easily conclude that, for a large enough n, the variable ϵ_n follows a centered Gaussian law of variance $\frac{\sigma^2}{n}$.

It is impossible to limit the error by using the previous theorem, since the variable ϵ_n is Gaussian of support infinite $\mathbb{R}$. The preceding remark allows us to construct intervals of confidence for the error estimation while doing the following way:

$$P(-a\frac{\sigma}{\sqrt{n}} < \epsilon_n < a\frac{\sigma}{\sqrt{n}}) = \mathbb{P}(|\epsilon_n| < a\frac{\sigma}{\sqrt{n}})$$

For instance for $a = 1.96$ and by the quantile of the normal law, we have:

$$\mathbb{P}(|\epsilon_n| < 1.96\frac{\sigma}{n}) \sim \mathbb{P}(|\aleph| < 1.96\frac{\sigma}{\sqrt{n}}) = 0.95$$

So, with a probability of 95, we get asymptotically:

$$|\epsilon_n| < 1.96\frac{\sigma}{\sqrt{n}}$$

The variance σ^2 intervenes in the increase of the error, it is therefore crucial to provide an estimator, which is easily done by the same draws $X_1, X_2, \cdots, X_n, \cdots$ of the variable X. The usual estimator $\hat{\sigma}_n^2$ of the variance is given by the following formula:

$$\hat{\sigma}_n^2 = \frac{1}{n-1} \sum_{i=1}^{n} (X_i - \bar{X}_n)^2$$

where $\bar{X}_n$ is the empirical estimator of the mean and because of the independence in the sample, the estimator $\hat{\sigma}_n^2$ is written:

$$\hat{\sigma}_n^2 = \frac{n}{n-1} (\frac{1}{n} \sum_{i=1}^{n} (X_i^2 - \bar{X}_n^2))$$

Regarding the properties of the new estimator, we can easily show that it converges to the variance when $\mathbb{E}(X^2) < +\infty$ i.e $\lim_{n \to \infty} \hat{\sigma}_n^2 = \sigma^2$, and $\hat{\sigma}_n^2$ is an unbiased estimator. When $\mathbb{E}(\hat{\sigma}_n^2) = \sigma_n^2$.

Gathering all the previous results, we arrive at an approximate confidence interval for the error by replacing σ with σ_n^2 and we will have:

$$I = \left[-1.96\frac{\hat{\sigma}_n^2}{\sqrt{n}}, 1.96\frac{\hat{\sigma}_n^2}{\sqrt{n}} \right]$$

Therefore considering a probability of 0.97, the expectation $E(X)$ belongs to the following interval:

$$I_c = \left[\bar{X}_n - 1.96\frac{\hat{\sigma}_n^2}{\sqrt{n}}, \bar{X}_n + 1.96\frac{\hat{\sigma}_n^2}{\sqrt{n}} \right].$$

Chapter 4

Numerical simulation and discussion

Contents

In this work more than 400 numerical simulations were carried out for various time steps varying between $\Delta t = 1/100$ and $\Delta t = 1/1000$ and for different numbers of particules varying between $N = 10^4$ and $N = 10^5$. These following simulation are the 20th smallest error on moment of order 0, their moment and exact moment of order 0.

4.1 Case of N = 10000 particles

n_t	$M_{0,N}$	$M_{0,N}\ exact$	**Error on** $M_{0,N}$
1/500	0.13262	0.13534	0.00271820
1/600	0.13631	0.13534	0.00097699
1/700	0.13629	0.13534	0.00095177
1/800	0.13581	0.13534	0.00047547
1/900	0.13576	0.13534	0.00042086
1/1000	0.13388	0.13534	0.00145430

TABLE 4.1 – Variation of the moment of order 0 and the exact moment of order 0 with the error corresponding to N = 10000 for Δt varying between $\Delta t = 1/500$ to $\Delta t = 1/1000$.

According to the numerical results presented in **Table 4.1**, we chose the most representative values of the error moments of order 0, in the case of N = 10000 particles for the time steps varying between $\Delta t = 1/400$ and $\Delta t = 1/900$.

FIGURE 4.1 – Comparison between analytical and numerical moment of order 0 (left) and the error on moment of order 0 corresponding to N = 10000 for $\Delta t = 1/400$.

FIGURE 4.2 – Comparison between analytical and numerical moment of order 0 (left) and the error on moment of order 0 corresponding to N = 10000 for $\Delta t = 1/900$.

4.2   Case of N = 20000 particles

n_t	$M_{0,N}$	$M_{0,N}\ exact$	**Error on** $M_{0,N}$
1/500	0.13588	0.13534	0.00544620
1/600	0.13446	0.13534	0.00087946
1/700	0.13490	0.13534	0.00043296
1/800	0.13040	0.13534	0.00129780
1/900	0.13531	0.13534	0.00003001
1/1000	0.13522	0.13534	0.00011716

TABLE 4.2 – Variation of the moment of order 0 and the exact moment of order 0 with the error corresponding to N = 20000 for Δt varying between $\Delta t = 1/500$ to $\Delta t = 1/1000$.

According to the numerical results presented in **Table 4.2**, we chose the most representative values of the error moments of order 0, in the case of N = 20000 particles for the time steps varying between $\Delta t = 1/900$ and $\Delta t = 1/1000$.

FIGURE 4.3 – Comparison between analytical and numerical moment of order 0 (left) and the error on moment of order 0 corresponding to N = 20000 for $\Delta t = 1/900$.

FIGURE 4.4 – Comparison between analytical and numerical moment of order 0 (left) and the error on moment of order 0 corresponding to N = 20000 for $\Delta t = 1/1000$.

4.3 Case of N = 30000 particles

n_t	$M_{0,N}$	$M_{0,N}$ exact	Error on $M_{0,N}$
1/500	0.13517	0.13534	0.00016810
1/600	0.13589	0.13534	0.00055008
1/700	0.13562	0.13534	0.00028020
1/800	0.13555	0.13534	0.00021587
1/900	0.13548	0.13534	0.00014087
1/1000	0.13395	0.13534	0.00138390

TABLE 4.3 – Variation of the moment of order 0 and the exact moment of order 0 with the error corresponding to N = 30000 for Δt varying between $\Delta t = 1/500$ to $\Delta t = 1/1000$.

According to the numerical results presented in **Table 4.3**, we chose the most representative values of the error moments of order 0, in the case of N = 30000 particles for the time steps varying between $\Delta t = 1/500$ and $\Delta t = 1/900$.
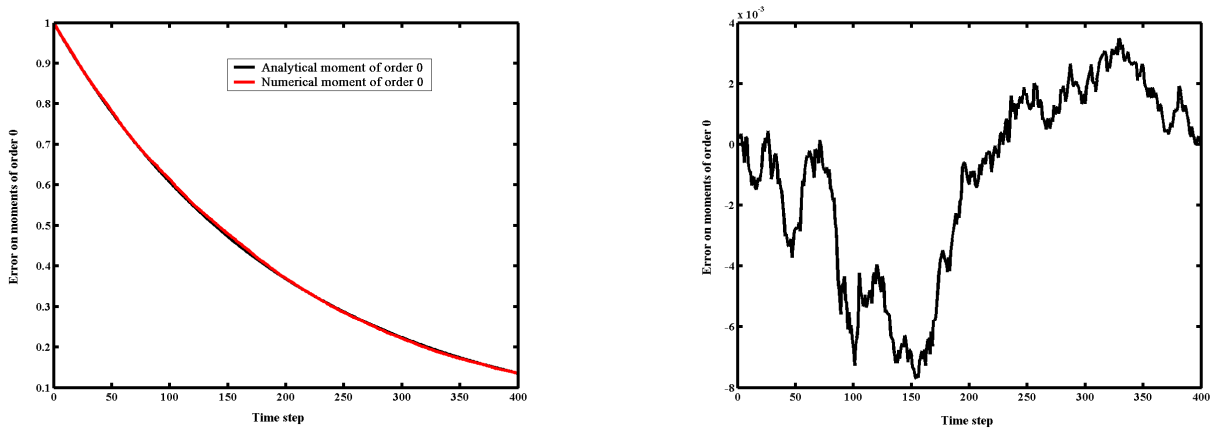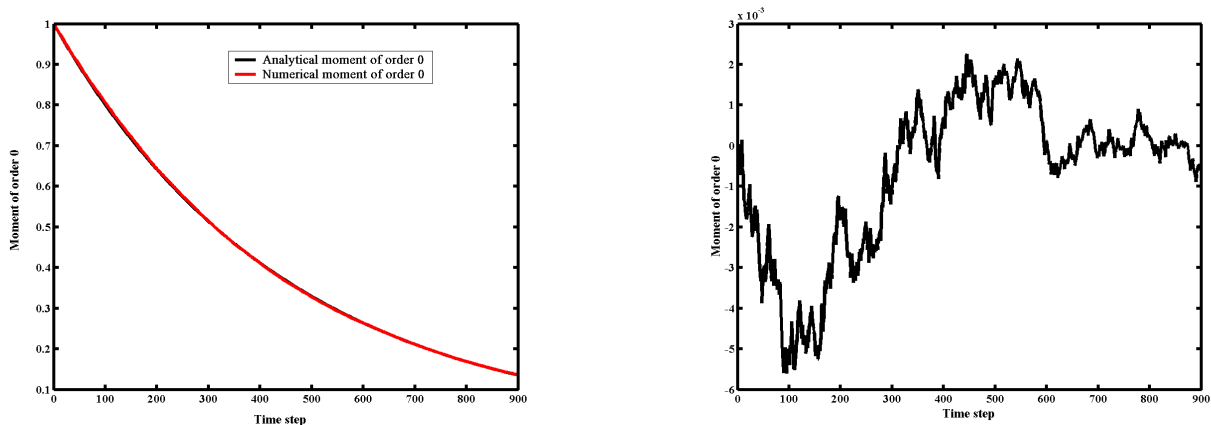

FIGURE 4.5 – Comparison between analytical and numerical moment of order 0 (left) and the error on moment of order 0 corresponding to N = 30000 for $\Delta t = 1/500$.

FIGURE 4.6 – Comparison between analytical and numerical moment of order 0 (left) and the error on moment of order 0 corresponding to N = 30000 for $\Delta t = 1/900$.

4.4   Case of N = 40000 particles

n_t	$M_{0,N}$	$M_{0,N}$ $exact$	**Error on** $M_{0,N}$
1/500	0.13501	0.13534	0.00032070
1/600	0.13607	0.13534	0.00073461
1/700	0.13672	0.13534	0.00138340
1/800	0.13679	0.13534	0.00145320
1/900	0.13705	0.13534	0.00171890
1/1000	0.13695	0.13534	0.00161370

TABLE 4.4 – Variation of the moment of order 0 and the exact moment of order 0 with the error corresponding to N = 40000 for Δt varying between $\Delta t = 1/500$ to $\Delta t = 1/1000$.

According to the numerical results presented in **Table 4.4**, we chose the most representative values of the error moments of order 0, in the case of N = 40000 particles for the time steps varying between $\Delta t = 1/200$ and $\Delta t = 1/400$.
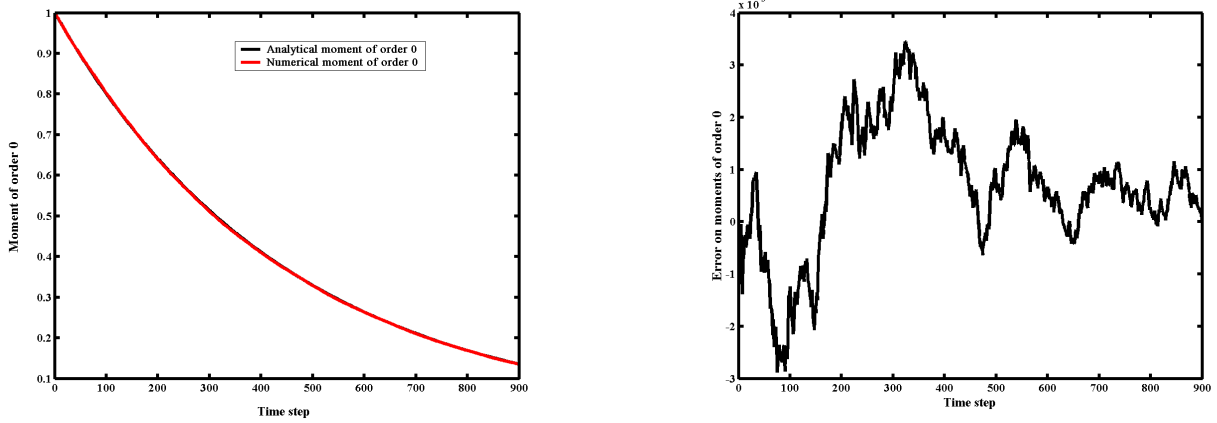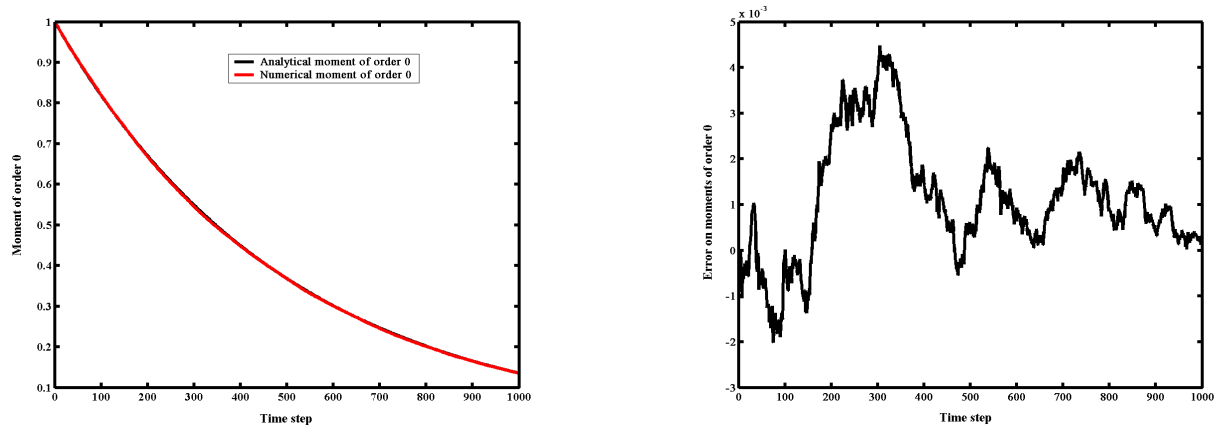
FIGURE 4.7 – Comparison between analytical and numerical moment of order 0 (left) and the error on moment of order 0 corresponding to N = 40000 for $\Delta t = 1/200$.

FIGURE 4.8 – Comparison between analytical and numerical moment of order 0 (left) and the error on moment of order 0 corresponding to N = 40000 for $\Delta t = 1/400$.

4.5 Case of N = 50000 particles

n_t	$M_{0,N}$	$M_{0,N}$ exact	Error on $M_{0,N}$
1/500	0.13625	0.13534	0.00091515
1/600	0.13657	0.13534	0.00123390
1/700	0.13637	0.13534	0.00103780
1/800	0.13608	0.13534	0.00074684
1/900	0.13588	0.13534	0.00054478
1/1000	0.13657	0.13534	0.00123660

TABLE 4.5 – Variation of the moment of order 0 and the exact moment of order 0 with the error corresponding to N = 50000 for Δt varying between $\Delta t = 1/500$ to $\Delta t = 1/1000$.

According to the numerical results presented in **Table 4.5**, we chose the most representative values of the error moments of order 0, in the case of N = 50000 particles for the time steps $\Delta t = 1/900$.

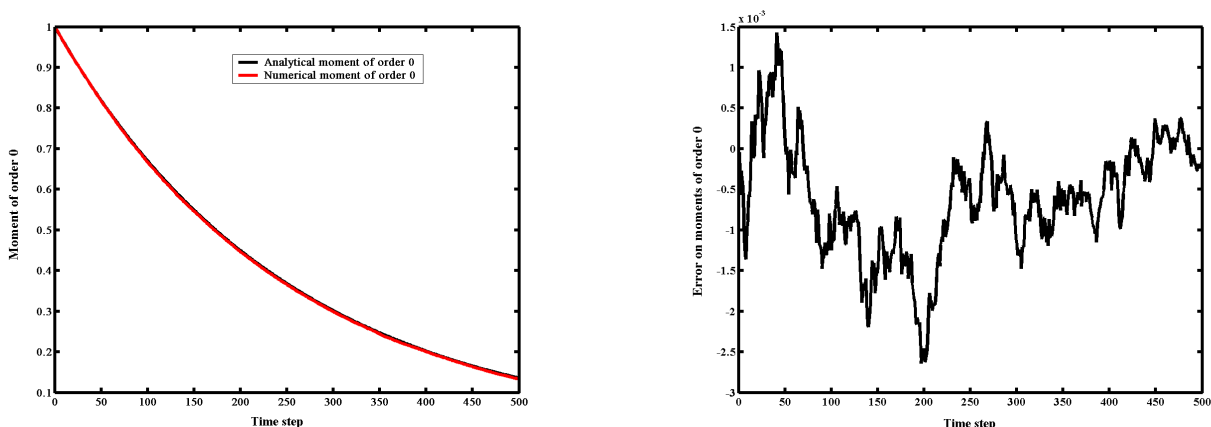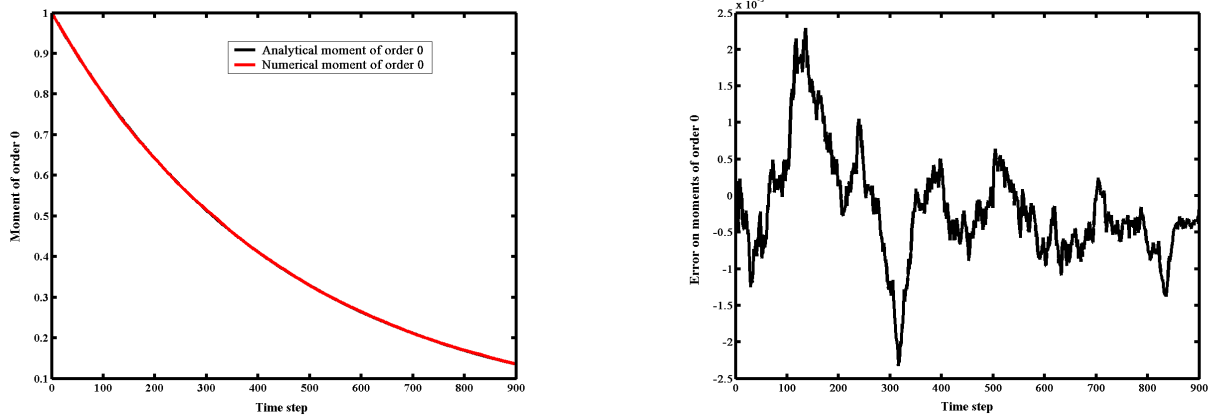FIGURE 4.9 – Comparison between analytical and numerical moment of order 0 (left) and the error on moment of order 0 corresponding to N = 50000 for $\Delta t = 1/900$.

4.6   Case of N = 60000 particles

n_t	$M_{0,N}$	$M_{0,N}$ exact	**Error on** $M_{0,N}$
1/500	0.13607	0.13534	0.00073337
1/600	0.13585	0.13534	0.00051664
1/700	0.13470	0.13534	0.00063904
1/800	0.13596	0.13534	0.00062229
1/900	0.13507	0.13534	0.00026736
1/1000	0.13443	0.13534	0.00090481

TABLE 4.6 – Variation of the moment of order 0 and the exact moment of order 0 with the error corresponding to N = 60000 for Δt varying between $\Delta t = 1/500$ to $\Delta t = 1/1000$.

According to the numerical results presented in **Table 4.6**, we chose the most representative values of the error moments of order 0, in the case of N = 60000 particles for the time steps $\Delta t = 1/900$.
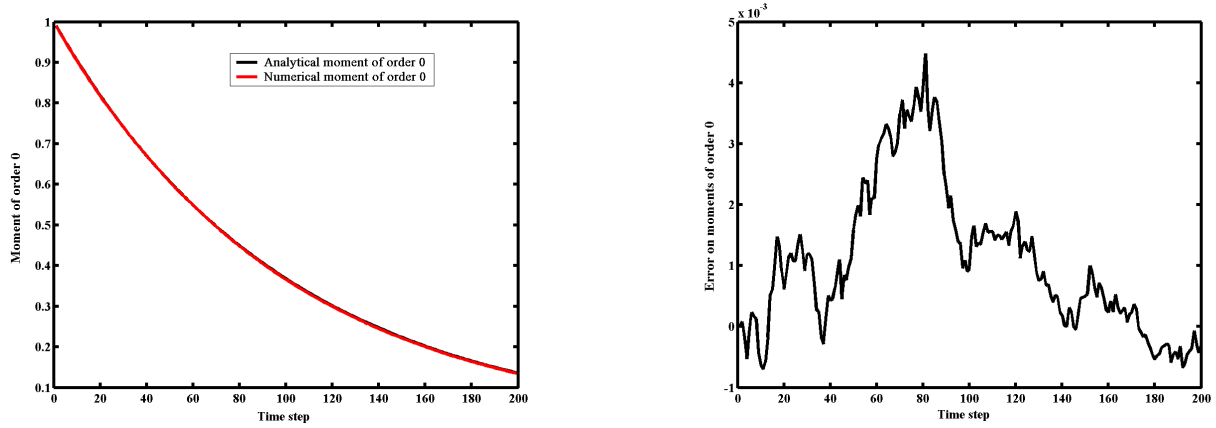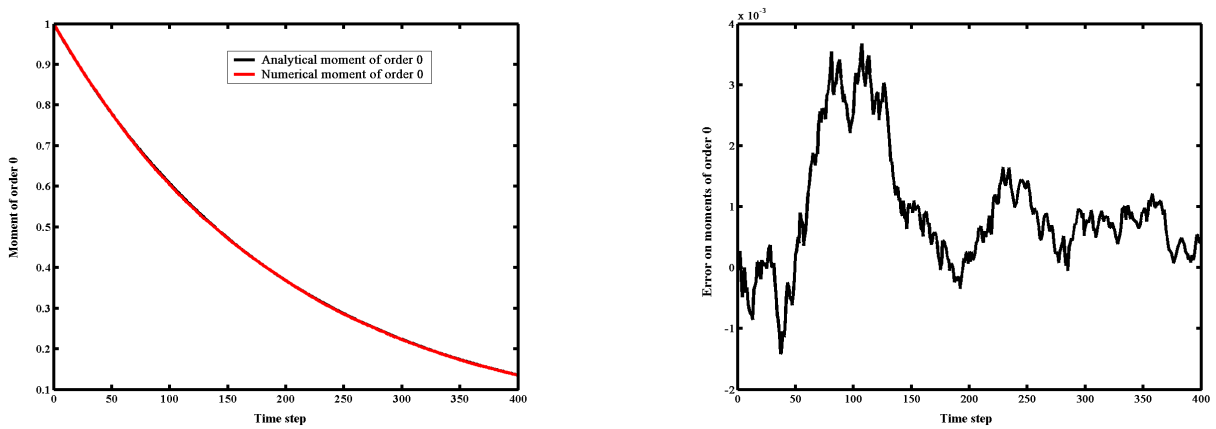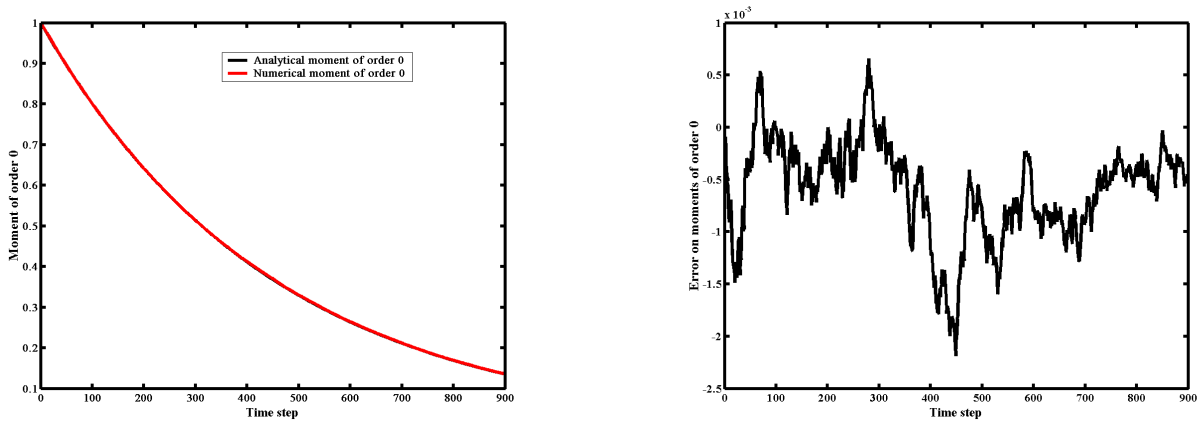

FIGURE 4.10 – Comparison between analytical and numerical moment of order 0 (left) and the error on moment of order 0 corresponding to N = 60000 for $\Delta t = 1/900$.

4.7   Case of N = 70000 particles

n_t	$M_{0,N}$	$M_{0,N}$ exact	Error on $M_{0,N}$
1/500	0.13365	0.13534	0.00168100
1/600	0.13535	0.13534	0.00001492
1/700	0.13608	0.13534	0.00074707
1/800	0.13565	0.13534	0.00031883
1/900	0.13689	0.13534	0.00155370
1/1000	0.13600	0.13534	0.00066006

TABLE 4.7 – Variation of the moment of order 0 and the exact moment of order 0 with the error corresponding to N = 70000 for Δt varying between $\Delta t = 1/500$ to $\Delta t = 1/1000$.

According to the numerical results presented in **Table 4.7**, we chose the most representative values of the error moments of order 0, in the case of N = 10000 particles for the time steps varying between $\Delta t = 1/300$ and $\Delta t = 1/800$.

FIGURE 4.11 – Comparison between analytical and numerical moment of order 0 (left) and the error on moment of order 0 corresponding to N = 70000 for $\Delta t = 1/300$.

FIGURE 4.12 – Comparison between analytical and numerical moment of order 0 (left) and the error on moment of order 0 corresponding to N = 70000 for $\Delta t = 1/600$.

FIGURE 4.13 – Comparison between analytical and numerical moment of order 0 (left) and the error on moment of order 0 corresponding to N = 70000 for $\Delta t = 1/800$.

4.8   Case of N = 80000 particles

n_t	$M_{0,N}$	$M_{0,N}$ $exact$	**Error on $M_{0,N}$**
1/500	0.13498	0.13534	0.00035911
1/600	0.13605	0.13534	0.00071821
1/700	0.13573	0.13534	0.00039756
1/800	0.13605	0.13534	0.00071434
1/900	0.13628	0.13534	0.00094227
1/1000	0.13468	0.13534	0.00065255

TABLE 4.8 – Variation of the moment of order 0 and the exact moment of order 0 with the error corresponding to N = 80000 for Δt varying between $\Delta t = 1/500$ to $\Delta t = 1/1000$.

According to the numerical results presented in **Table 4.8**, we chose the most representative values of the error moments of order 0, in the case of N = 80000 particles for the time steps varying between $\Delta t = 1/400$ and $\Delta t = 1/700$.
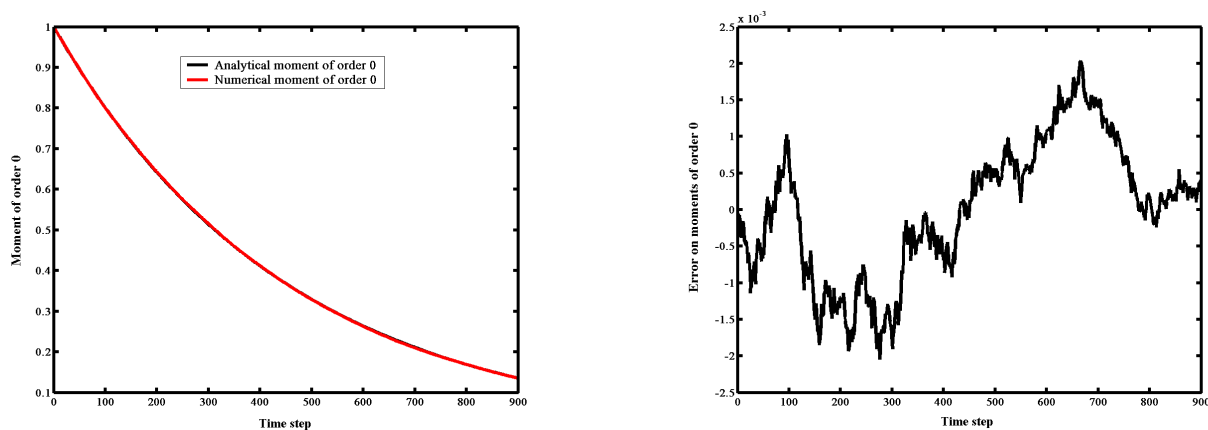

FIGURE 4.14 – Comparison between analytical and numerical moment of order 0 (left) and the error on moment of order 0 corresponding to N = 80000 for $\Delta t = 1/400$.
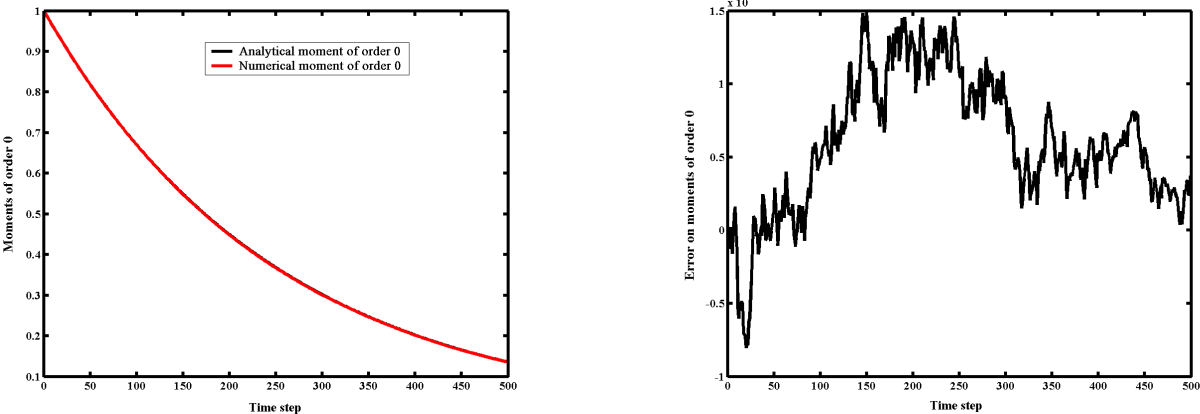
FIGURE 4.15 – Comparison between analytical and numerical moment of order 0 (left) and the error on moment of order 0 corresponding to N = 80000 for $\Delta t = 1/500$.
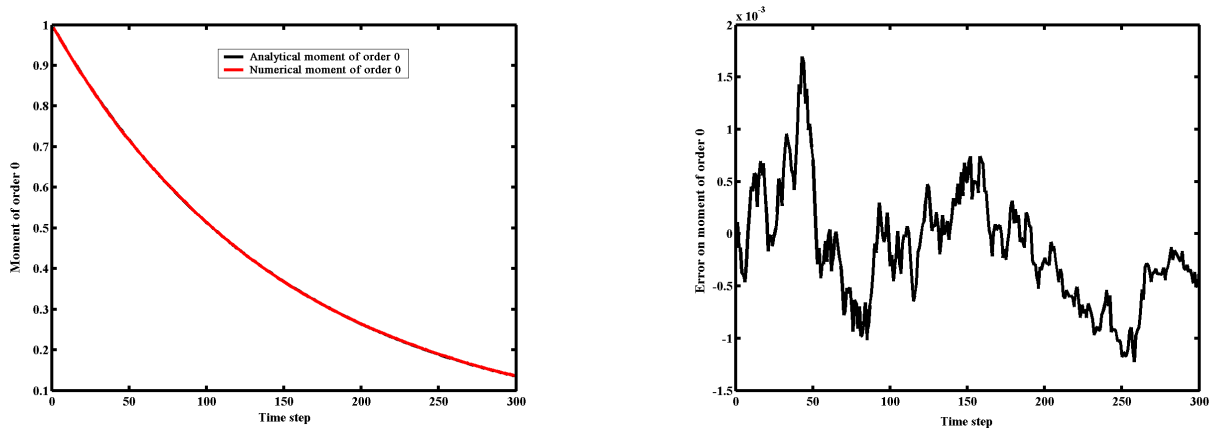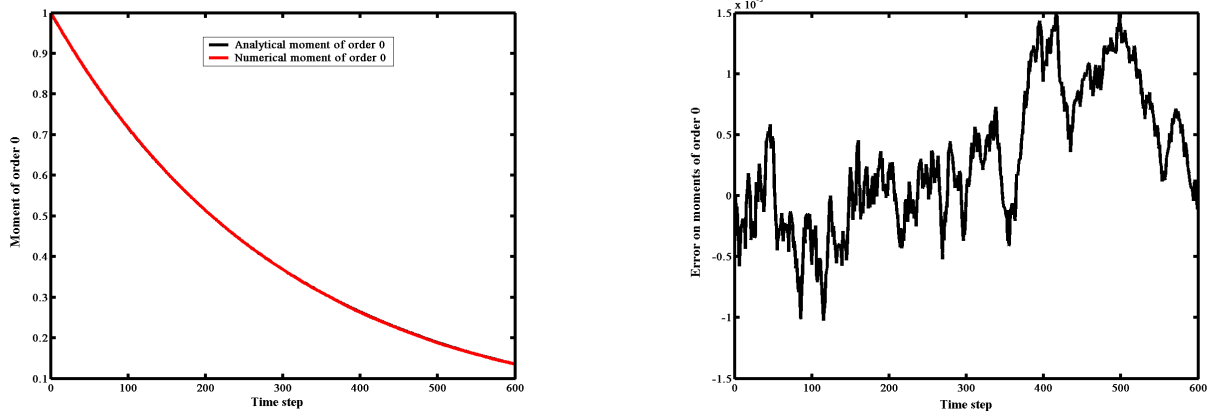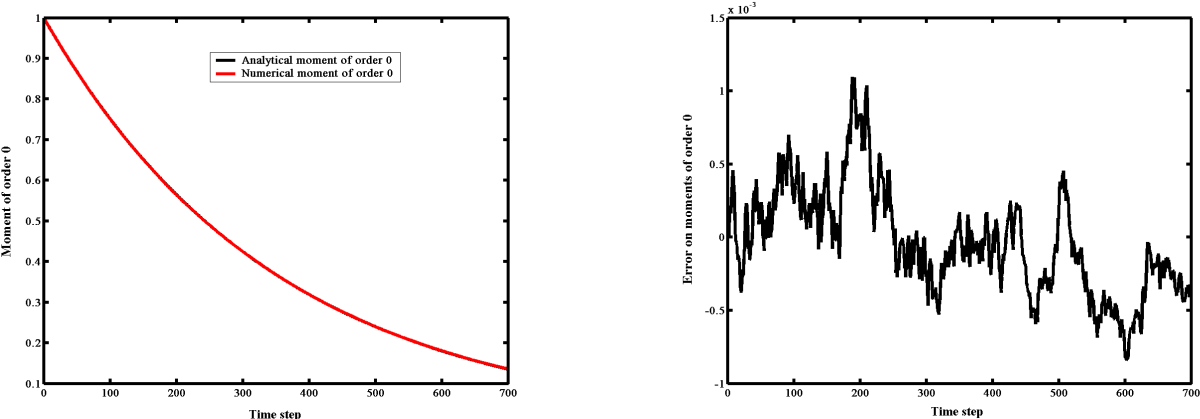

FIGURE 4.16 – Comparison between analytical and numerical moment of order 0 (left) and the error on moment of order 0 corresponding to N = 80000 for $\Delta t = 1/700$.

4.9   Case of N = 90000 particles

n_t	$M_{0,N}$	$M_{0,N}$ exact	**Error on** $M_{0,N}$
1/500	0.13599	0.13534	0.00065943
1/600	0.13477	0.13534	0.00056633
1/700	0.13483	0.13534	0.00050770
1/800	0.13519	0.13534	0.00014123
1/900	0.13514	0.13534	0.00019237
1/1000	0.13536	0.13534	0.00002918

TABLE 4.9 – Variation of the moment of order 0 and the exact moment of order 0 with the error corresponding to N = 90000 for Δt varying between $\Delta t = 1/500$ to $\Delta t = 1/1000$.

According to the numerical results presented in **Table 4.9**, we chose the most representative values of the error moments of order 0, in the case of N = 90000 particles for the time steps varying between $\Delta t = 1/800$ and $\Delta t = 1/1000$.
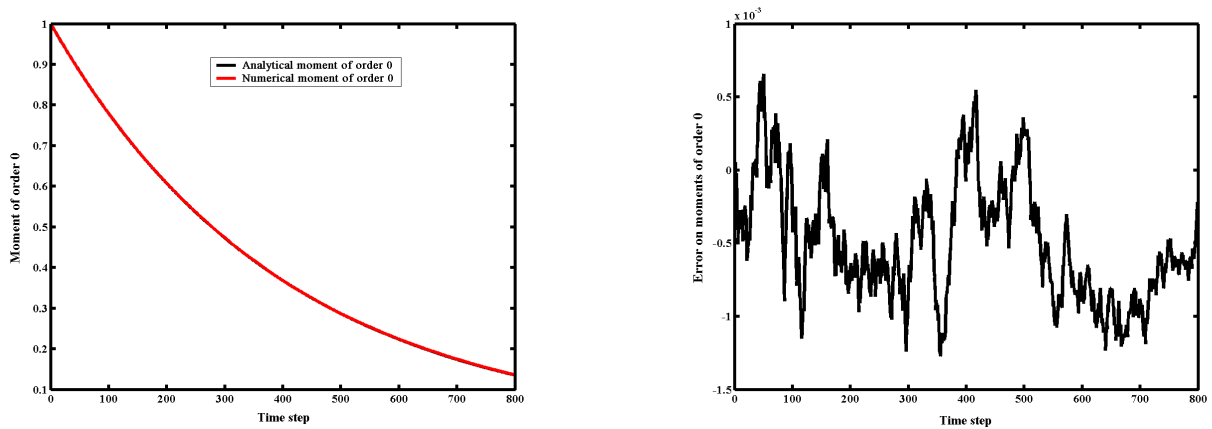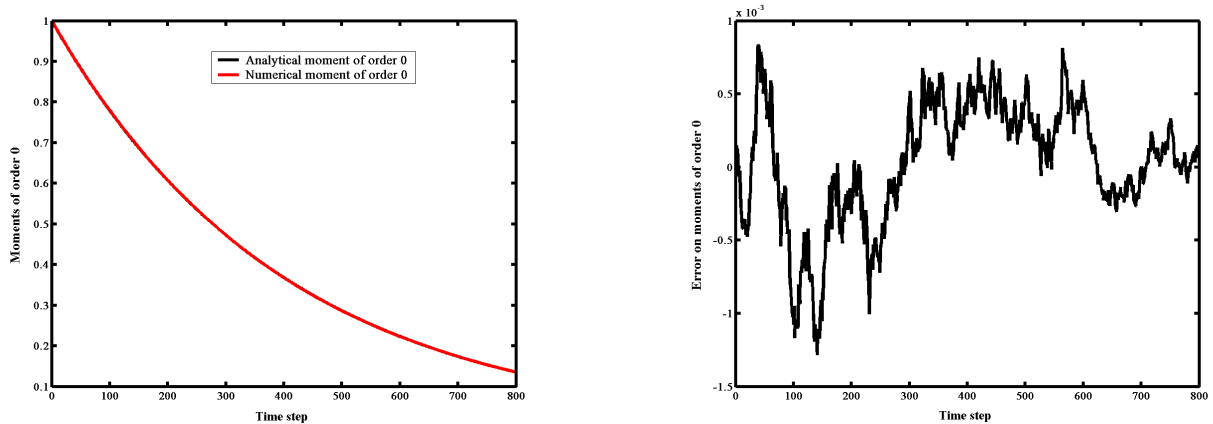

FIGURE 4.17 – Comparison between analytical and numerical moment of order 0 (left) and the error on moment of order 0 corresponding to N = 90000 for $\Delta t = 1/800$.
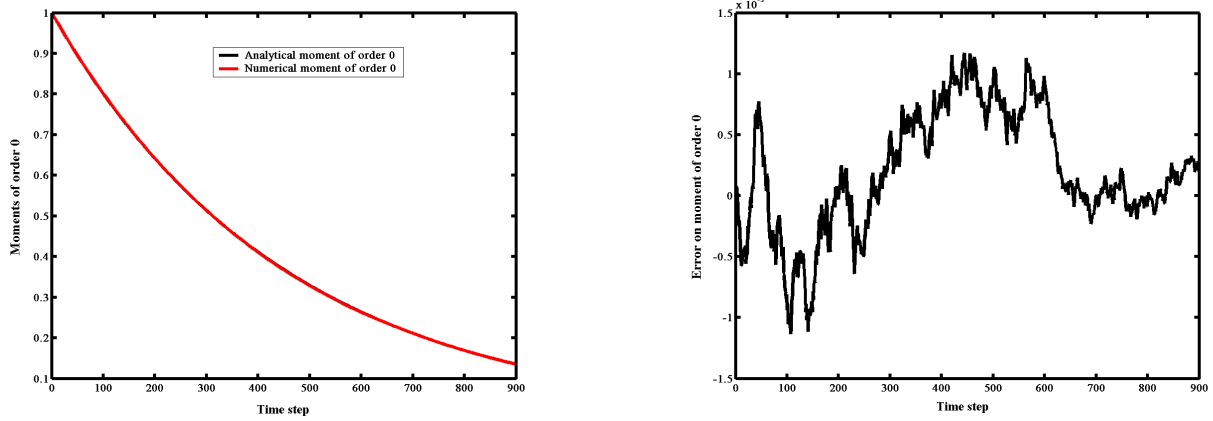
FIGURE 4.18 – Comparison between analytical and numerical moment of order 0 (left) and the error on moment of order 0 corresponding to N = 90000 for $\Delta t = 1/900$.
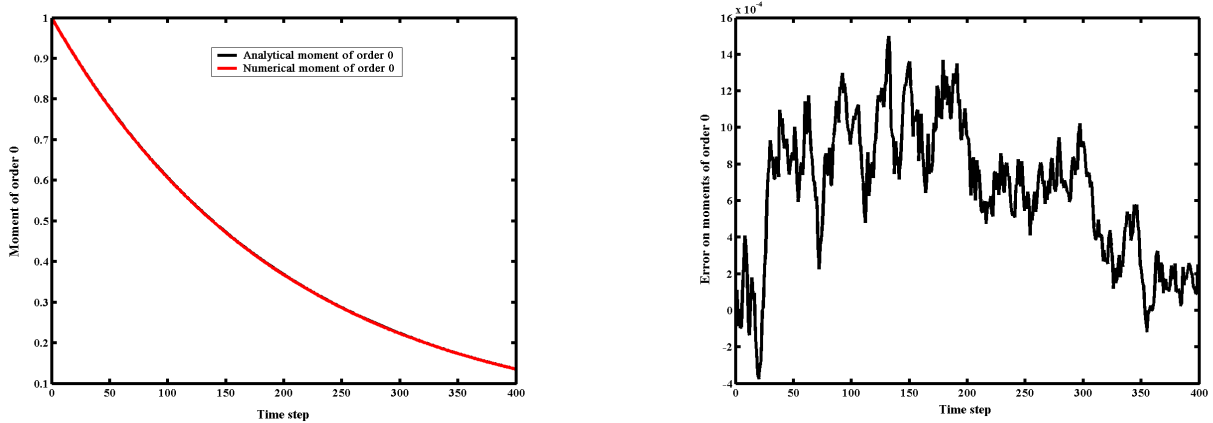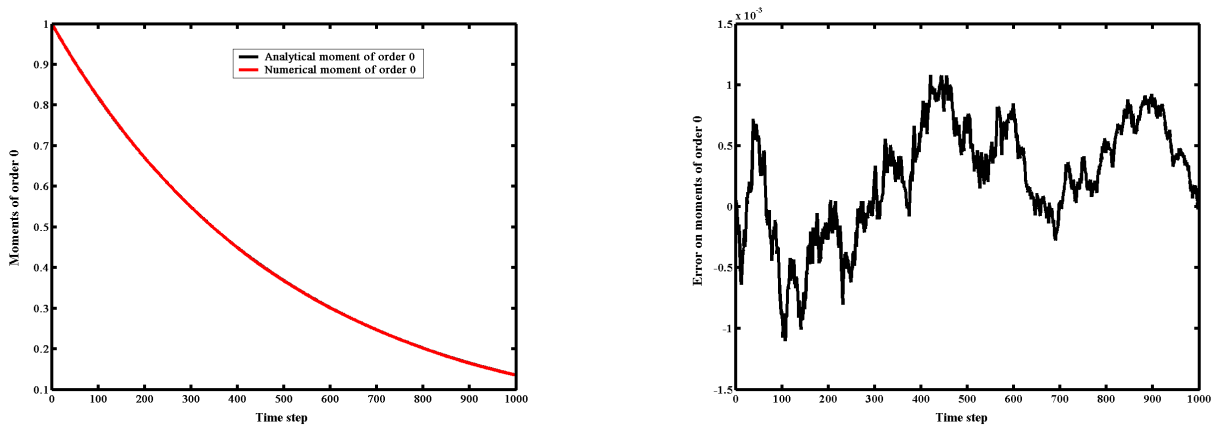

FIGURE 4.19 – Comparison between analytical and numerical moment of order 0 (left) and the error on moment of order 0 corresponding to N = 90000 for $\Delta t = 1/1000$.

4.10 Case of N = 10000 particles

n_t	$M_{0,N}$	$M_{0,N}$ exact	Error on $M_{0,N}$
1/500	0.13434	0.13534	0.00099828
1/600	0.13451	0.13534	0.00082986
1/700	0.13385	0.13534	0.00148040
1/800	0.13425	0.13534	0.00108500
1/900	0.13439	0.13534	0.00094474
1/1000	0.13456	0.13534	0.00077086

TABLE 4.10 – Variation of the moment of order 0 and the exact moment of order 0 with the error corresponding to $N = 10^5$ for Δt varying between $\Delta t = 1/500$ to $\Delta t = 1/1000$.

According to the numerical results presented in **Table 4.10**, we chose the most representative values of the error moments of order 0, in the case of N = 10000 particles for the time steps $\Delta t = 1/300$.
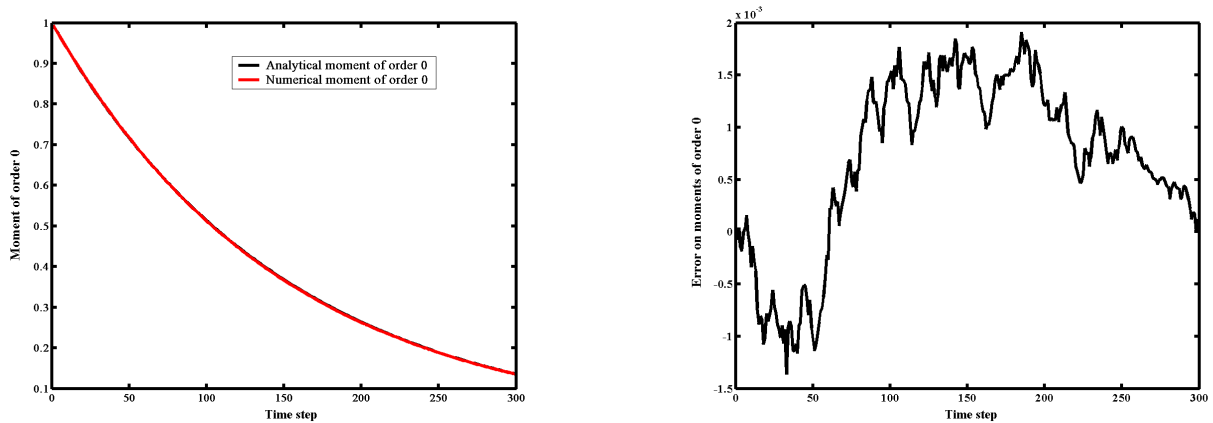
FIGURE 4.20 – Comparison between analytical and numerical moment of order 0 (left) and the error on moment of order 0 corresponding to N = 100000 for $\Delta t = 1/300$.

The following simulations shows the validity of the Smoluchowski theory approach with comparing results of computer.

Conclusion

In this work, we have analysed an approach for solving Smoluchowski's coagulation equation using the Monte Carlo method in order to simulate the aggregation of polymers employed in the waste water process treatment. Our study provides numerical evidence that the numerical method seems to be accurate approximating the zeroth moment representing the particle number concentration, which decreases with the growth of the particle size. We have shown that the time step influence the error on moment in such a manner that considering a certain number of particles, more the time step decreases, more the error on moments of order 0 decreases.

Among the various perspectives of this work, we cite the aerosol physics coalescence problems. In fact, Atmospheric aerosols are solid or liquids particles suspended in atmosphere and has a profound effect on our lives. It affects global climate and personal health. Aerosol particles vary in size, concentration and distribution in space and time. The aerosol concentration in atmosphere is variable due to the heterogeneity of chemical compositions and sources, interactions with clouds and solar and tell-uric radiation. One of the essential problems of aerosol physics is coalescence due to microphysical transformation processes. The droplet rate growth with coalescence governed by the collection efficiency. Two drops of fusion are forming a composite. If the average distance between the drops is less than a threshold value or a coalescence limit, the compound drop will touch a neighboring drop. Other coalescence follows if the drops are close enough between them. Coalescences can thus be chained. We intend to study the evolution of the numerical concentration as a function of the particle size, better known under the coagulation rate.

Another goal consiste of correcting the second order moment which is the total light scattered which increases with the growth of the particle size and polydisperity.

Bibliography

[1] E. CEPEDA (2013), *Contribution to the probabilistic and numerical study of homogeneous Coagulation- Fragmentation equations*, Probability [math.PR], Université Paris-Est.

[2] R. BRAGA MORUZZI, S. CONCEIÇÃO DE OLIVEIRA (2012), *Mathematical modeling and analysis of the flocculation process in chambers in series*, Springer-Verlag.

[3] M. ROGER (2008), *Méthodes de Monte-Carlo*, Service de Physique de l'Etat Condensé CEA Saclay.

[4] M. YU, M. SEIPENBUSCH, J. YANG, H. JIN (2014), *A New Analytical Solution for Solving the Smoluchowski Equation Due to Nanoparticle Brownian Coagulation for Non-Self-Preserving System*, Aerosol and Air Quality Research, Taiwan Association for Aerosol Research ISSN, China.

[5] A. HAMMOND (2009), *Moment Bounds for the Smoluchowski Equation and their Consequences*, New York University and Fraydoun Rezakhanlou†, UC Berkeley.

[6] A. HAMMOND (2009), *Moment Bounds for the Solutions of the Smoluchowski Equation with Coagulation and Fragmentation* , UC Berkeley Department of Mathematics Berkeley.

[7] M. NORMANDIN (2005), *Étude sur la clarification d'une suspension de boue rouge et de liqueur Bayer par floculation* , Mémoire présenté à l'université du Québec à Chicoutimi comme exigence partielle de la maîtrise en ingénierie.

[8] G. LARCHER, J. KEPLER, F. PILLICHSHMMER, A. WINTERHOF, C. XING (2014), *Applied Algebra and Number Theory*, University Linz, Austrian Academy of Sciences, Nanyang Technological University, Singapore.

[9] S. FERNANDO TORREALBA (2010), *A Continuous Mathematical Model of the One-Dimensional Sedimentation Process of Flocculated Sediment Particles*, University of Kentucky UKnowledge.

[10] D. AMEUR (2008), *Modélisation analytique et simulation numérique par la méthode de Monte Carlo d'un écoulement de gaz dans des micro-canaux*, Thèse de Doctorat, Institut Jean Le Rond d'Alembert, Sorbonne Universités-Université Pierre et Marie Curie, France.

[11] J. DIB, D. AMEUR, S. BELALIA AND I. RASPO (2018), *Statistical Study for Colloidal Suspensions Aggregation*, Proceeding dans CIEMEAP, Constantine, 29-30 Avril.

[12] D. AMEUR, J. DIB, S. BELALIA (2018), *Modeling and Simulation of Chemical Treatment for Urban Waste Water Process*, Proceeding dans ISyMC, Boumerdès, 19-20 Mars.

[13] M.V. SMOLUCHOWSKY (1917),*Versuch einer mathematischen Theorie der Koagulationskinetik kolloider Lösnngen (original paper)*.

[14] M. JEAN PERRIN (1909), *Brownian movement and molecular reality*, Faculté des sciences, Université de Paris.

[15] J. F. LE GALL (2013), *Mouvement brownien*, Martingales et calcul stochastique, mathématiques et applications.

[16] A. GULDBERG (1922), *Un théorème du calculs des probabilités*, Nouvelle annales de mathématiques, 5e série, tome 1, p.251-254.

[17] A. THILL (1999), *Agrégation des particules : structure, dynamique et simulation. Application au cas d'un écoulement stratifié : l'estuaire du Rhône*, Thèse doctorat de l'université d'Aix-Marseille 3, spécialité géo-sciences.

[18] M. PATY (2002), *Poincaré, Langevin et Einstein*, Epistemologiques, n° 1-2, pp.33-73.

[19] A. EINSTEIN, *Investigations on the theory of the brownian movement*, Edited with notes by R. Furth, Translated by A. D. Cowper, DOVERPUBLICATIONS, INC.

[20] C. MICHAUT (2005), *Les multiples vies de Paul Langevin*, Présence de l'histoire, Pour la science, N° 355.

[21] R. FAKHEREDDINE (2013), *Méthodes de Monte Carlo stratifiées pour l'intégration et la simulation numériques*, Thèse de Doctorat de l'Université de Grenoble.

[22] W. JOHN , C. BUCKLEYB , E. JACOBSC , RD. SANDERSONC (2002), *Synthesis and use of PolyDADMAC for water purification*, Paper presented at the Biennial Conference of the Water Institute of Southern Africa (WISA), Durban, South Africa.

[23] S. AL-ASHEH, A. AIDAN (2017), *Operating Conditions of Coagulation-Flocculation Process for High Turbidity Ceramic Wastewater*, Department of Chemical Engineering, American University of Sharjah, Sharjah, UAE, J. Water Environ, Nanotechnol, UAE.

[24] P. CARR (2017), *Bounded Brownian Motion*, Department of Finance and Risk Engineering, Tandon School of Engineering, NYU, 12 MetroTech Center, Brooklyn, NY 11201, USA.

[25] B. BRUCE, W. WALTER, W. TSCHARNUTER, D. FAIRHURST (1993), *Bounded Brownian Motion*, Brookhaven Instruments Corporation Holtsville, NY 11742 USA, paper presented at the Canadian Mineral Analysts Meeting, held in Winnipeg, Manitoba, Canada.

Certificate of participation to international conference and proceedings

243

Fourth International Conference on Energy, Materials, Applied Energetics and Pollution (ICEMAEP'18)

Laboratoire de Mécanique Lagh-Univ

LAEP

GRESPI
Groupe de Recherche En Sciences Pour l'Ingenieur

جامعة الإخوة منتوري قسنطينة 1
Université des Frères
Mentouri – Constantine 1

Organized on the 29th and the 30th of April 2018 by:

The Applied Energetics and Pollution Laboratory (LAEP), Mentouri Brothers' Constantine 1 University, Algeria
The Laboratory of Advanced Technological Applications (LATA), Mentouri Brothers' Constantine 1 University, Algeria

in collaboration with:

The GRESPI Laboratory, University of Champagne Ardennes, France
The LM Laboratory, University of Laghouat, Algeria
The LTA Laboratory, University of Boumerdes, Algeria
The SDIRL laboratory, University of Ouargla, Algeria

Tel : 0773403523, Fax :031866534, Email : ciemeap2018@gmail.com

CERTIFICATE OF PARTICIPATION

The organizing committee of the 4th International Conference on Energy, Materials, Applied Energetics and Pollution ICEMAEP'18 held on 29th and 30th of April 2018 in Constantine in Algeria, certifies that: **Soumia Belalia** has successfully participated in the conference by presenting the following paper:

Title : **STATISTICAL STUDY FOR COLLOIDAL SUSPENSIONS COAGULATION**

Authors: **Djilali Ameur, Joanna Dib, Soumia Belalia, Isabelle Raspo**

The Conference Chairman
Pr. Mahfoud KADJA
Prof. M. KADJA
Conference Chairman

ICEMAEP'18
April 29-30,2018
Constantine-Algeria
Conference on Energy, Materials, Applied Energetics and Pollution * 4th International

RSDT

Aigle

sonelgaz

Briquetterie Tidjelabine

Tidjelabine steel

MADi Laboratoire

ATRST

Sponsors :

République Algérienne Démocratique et Populaire
Ministère de l'Enseignement Supérieur et de la Recherche Scientifique
Direction Générale de la Recherche Scientifique et du Développement Technologique
Université M'Hamed Bougara Boumerdès
Faculté des Sciences
Département Chimie

Certificate of Participation

This is to certify that

DIB Joanna

Has successfully participated in the

International Symposium on Materials Chemistry

19-21 March 20**18**, Boumerdes - Algeria

With an Oral presentation entitled:

"Modeling and Simulation of Chemical Treatment for Urban Waste Water Process "

Co-authors: Djilali Ameur, Soumia Belalia

Dr IREKTI Amar
ISyMC Chair

ABSTRACT

Over the years, because of fast growth of population and industrial activities, we have increasingly polluted our waters. Conventional water treatment processes become inadequate with the identification of new contaminants in the water. To overcome these challenges, a particular emphasis is accorded to the implementation of environmentally, eco-friendly and less-energy technologies for water treatment processes. In this context, we investigate wether new chemical treatments employing organic polymers are efficient enough to provide green solutions for waste water recycling. We focus our attention on stabilized colloidal suspensions that show no sedimentation rate. In order to destabilize these colloids, two mechanisms are mainly involved: coagulation and floculation. These mechanisms depend on the aggregation rate between particles modelised by the Smoluchowski's coagulation equation. In this paper, we study the number concentration of coagulated particles and we show more the time step decreases, more the error on moments of order 0 decreases for a certain number of particles.

Keywords: *Polymers, colloids, simulation, Smoluchowski equations, Monte Carlo method.*

ملـخص

على مر السنين وبسب النمو السريع للكثافة السكانية والأنشطة الصناعية، قمنا بتلويث مياهنا. مع تحديد الملوث الجديد في الماء أصبحت عمليات المعالجة التقليدية للمياه غير متوفرة. للتغلب على هذه التحديات، يتم التركيز بشكل خاص على تنفيذ تقنيات صديقة للبيئة تستهلك طاقة أقل في عمليات معالجة المياه. في هذا السياق نحن بصدد التحقيق فيما إذا كانت المعالجة الكيميائية الجديدة باستخدام البوليمرات العضوية فعالة بما يكفي لتوفير حلول صديقة للبيئة لإعادة تدوير المياه المستعملة. نركز انتباهنا على تعليق الغروية المستقرة التي لا تظهر أي معدل ترسيب. من أجل زعزعة هذه الغرويات هناك آليتان رئيسيتان ز التخثر والترويب. تعتمد هذه الآليات على معدل التجميع بين الجزيئات التي تم تصميمها بمعادلة التخثر سمولشوسكي. في هده المذكرة، ندرس تركيز عدد الجسيمات المتخثرة، ونبين أنه كلما انخفضت وتيرة الزمن، انخفضت معها نسبة الخطأ في لحظات الترتيب 0 لعدد معين من الجسيمات.

كلمات مفتاحية: *البوليمرات، الغرويات، المحاكاة، معادلات سمولشوسكي، طريقة مونت كارلو.*

RÉSUMÉ

Au fil des années, en raison de la croissance rapide de la population et des activités industrielles, nous avons de plus en plus pollué nos eaux. Les procédés classiques de traitement des eaux usées deviennent inadéquats avec l'identification de nouveaux contaminants dans l'eau. Pour surmonter ces défis, un accent particulier est mis sur la mise en œuvre de technologies respectueuses de l'environnement, et moins énergivores pour les procédés de traitement de l'eau. Dans ce contexte, nous étudions si de nouveaux traitements chimiques utilisant des polymères organiques sont suffisamment efficaces pour fournir des solutions écologiques pour le recyclage des eaux usées. Nous concentrons notre attention sur les suspensions colloïdales stabilisées qui ne montrent aucun taux de sédimentation. Afin de déstabiliser ces colloïdes, deux mécanismes sont principalement impliqués : la coagulation et la floculation. Ces mécanismes dépendent du taux d'agrégation entre les particules modélisées par l'équation de coagulation de Smoluchowski. Dans ce mémoire, nous étudions la concentration en nombre de particules coagulées et nous montrons que plus le pas de temps diminue, plus l'erreur sur les moments d'ordre 0 diminue pour un certain nombre de particules.

Mots-clés : *Polymères, colloïdes, simulation, équations de Smoluchowski, méthode de Monte Carlo.*